



Michigan Technological University
Digital Commons @ Michigan
Tech

Dissertations, Master's Theses and Master's Reports
- Open

Dissertations, Master's Theses and Master's Reports

2011

Post processing of multiple GPS receivers to enhance baseline accuracy

Eddy H. Trinklein
Michigan Technological University

Copyright 2011 Eddy H. Trinklein

Recommended Citation

Trinklein, Eddy H., "Post processing of multiple GPS receivers to enhance baseline accuracy", Master's Thesis, Michigan Technological University, 2011.
<http://digitalcommons.mtu.edu/etds/414>

Follow this and additional works at: <http://digitalcommons.mtu.edu/etds>



Part of the [Mechanical Engineering Commons](#)

POST PROCESSING OF MULTIPLE GPS RECEIVERS TO ENHANCE
BASELINE ACCURACY

By

Eddy H. Trinklein

A THESIS

Submitted in partial fulfillment of the requirements for the degree of

MASTER OF SCIENCE

(MECHANICAL ENGINEERING)

MICHIGAN TECHNOLOGICAL UNIVERSITY

2011

Copyright © 2011 Eddy H. Trinklein

This thesis, "Post Processing Of Multiple GPS Receivers To Enhance Baseline Accuracy," is hereby approved in partial fulfillment for the requirements for the Degree of MASTER OF SCIENCE IN MECHANICAL ENGINEERING.

Department of Mechanical Engineering – Engineering Mechanics

Advisor: _____
Dr. Gordon G. Parker

Department Chair: _____
Professor William W. Predebon

Date: _____

Contents

<i>List of Figures</i>	xi
<i>List of Tables</i>	xiii
<i>Acknowledgments</i>	xv
<i>Abstract</i>	xvii
<i>1. Introduction</i>	1
1.1 GPS Operational Components	2
1.1.1 Space Segment	2
1.1.2 User Segment	2
1.1.3 Control Segment	3
1.2 GPS Satellite signals	4
1.3 The GPS Concept	4
1.3.1 Two Dimensional Case	5

1.3.2	Three Dimensional Case	5
1.4	GPS Error Sources	9
1.4.1	Clock Errors	9
1.4.2	Receiver Noise	9
1.4.3	Ephemeris Errors	11
1.4.4	Atmospheric Effects	11
1.4.5	Multipath Interference	12
1.4.6	Electrical Interference	12
1.4.7	GPS Error Summary	13
1.5	GPS accuracy	13
1.5.1	Standard Positioning Service accuracy	13
1.5.2	Differential GPS accuracy	14
1.5.3	WAAS DGPS accuracy	14
1.5.4	Real Time Kinematic accuracy	15
1.5.5	Post Processing Techniques	16
1.6	Proposed Post Processing Algorithm	16
2.	<i>Post Processing Algorithm</i>	19
2.1	Vincenty's Formulae for Determining Distance Between Two Points	19

2.1.1	Vincenty's Direct Method	20
2.1.2	Vincenty's Inverse Method	23
2.2	Receiver Coordinate Translation	24
2.3	Truncated Mean	29
2.4	Moving Average Filtering	31
3.	<i>Hardware Implementation</i>	36
3.1	Hardware Components	36
3.2	Physical Dimensions of Multiple GPS System	40
3.3	Data Recording Program	42
3.3.1	RS-232 Communication	42
3.3.2	Analog and Digital I/O	42
3.3.3	Parsing GPS Data Strings	42
3.3.4	Automatic Data File Handling	44
3.3.5	User Display	45
4.	<i>GPS Testing and Algorithm Results</i>	47
4.1	Short Duration Stationary Testing	47
4.1.1	Test Objective	47
4.1.2	Test Plan and Procedure	48

4.1.3	Short Duration Results	50
4.2	Long Duration Stationary Testing	55
4.2.1	Test Objective	55
4.2.2	Test Plan and Procedure	55
4.2.3	Long Duration Results	55
4.3	Mobile Testing	57
4.3.1	Test Objective	57
4.3.2	Test Plan and Procedure	57
4.3.3	Mobile Results	58
5.	<i>Summary, Conclusions, and Future Work</i>	67
5.1	Summary	67
5.2	Conclusions	68
5.3	Future Work	69
<i>References</i>	71
<i>Appendix A: Raw Data Figures</i>	73

List of Figures

1.1	GPS Orbits	3
1.2	Two dimensional user position.	5
1.3	Three dimensional user position.	7
1.4	Mobile Data comparing Raw Latitudes vs. Longitudes.	10
1.5	Baseline Distance between Two GPS Clusters.	16
2.1	ECEF and ENU Coordinate System Relationship	25
2.2	Coordinate Translation of a Single Receiver	26
2.3	Translation Algorithm Error as a Function of Azimuth, Distance 0.127 meters	28
2.4	Determining Azimuth between two GPS Clusters	29
2.5	Moving Average Filter Frequency Response as a Function of Number of Data Points Used, N	32
2.6	Mobile Test 1, 4.48 m Baseline, Effect of Number of Averaged Data Points on Rover Coordinates , Truncated Mean Percent = 50	33

2.7	Mobile Test 1, 4.48 m Baseline, Effect of Number of Averaged Data Points on Baseline, Truncated Mean Percent = 50	34
2.8	Averaging and Filtering Algorithm Flowchart	35
3.1	Data Collection Block Diagram for each Cluster	40
3.2	Actual Equipment Setup for each Cluster	41
4.1	Short Duration Stationary Test Setup	49
4.2	Actual Short Duration Stationary Test	49
4.3	Map Showing Locations where Stationary and Mobile Data was Collected .	50
4.4	Time Average Short Duration Stationary Test, Baseline Error, Test 1, 25 Nov 2010, Start Time = 190417 UTC	51
4.5	Time Averaged Short Duration Stationary Test, Baseline Error, Test 2, 25 Nov 2010, Start Time = 213618 UTC	53
4.6	Time Averaged Short Duration Stationary Test, Baseline Error, Multiple GPS System, Tests 1 - 2	54
4.7	Long Duration Stationary Test, 45.72 meter Baseline, 29 Nov 2010, Start Time = 161853 UTC	56
4.8	Actual Mobile Test Vehicle	58
4.9	Mobile Test Vehicle Setup	59
4.10	Mobile Test 1, Multiple GPS System and Javad RTK Comparison, 4.48 m Baseline, 29 Dec 2010, Start Time = 193648 UTC	60

4.11	Mobile Test 1, Multiple GPS System and Javad RTK Comparison, 4.48 m Baseline, 29 Dec 2010, Start Time = 193648 UTC	61
4.12	Mobile Test 2, Multiple GPS System and Javad RTK Comparison, 4.48 m Baseline, 29 Dec 2010, Start Time = 22502 UTC	62
4.13	Mobile Test 3, Multiple GPS System and Javad RTK Comparison, 4.48 m Baseline, 30 Dec 2010, Start Time = 150311 UTC	63
4.14	Mobile Test 1, Absolute Error Comparison, 4.48 m Baseline, 29 Dec 2010, Start Time = 193648 UTC	64
4.15	Mobile Test 2, Absolute Error Comparison, 4.48 m Baseline, 29 Dec 2010, Start Time = 22502 UTC	64
4.16	Mobile Test 3, Absolute Error Comparison, 4.48 m Baseline, 30 Dec 2010, Start Time = 150311 UTC	65
4.17	Mobile Test Comparison of Multiple GPS system,Tests 1 - 3, 4.48 m Baseline	65
A.1	Short Duration Stationary, Raw Baselines, 7.62 - 45.72 meters, Test 1 . . .	74
A.2	Short Duration Stationary, Baseline comparison, 7.62 - 45.72 meters, Test 1 . . .	74
A.3	Short Duration Stationary, Raw Baselines 7.62-45.72 m, Test 2	75
A.4	Short Duration Stationary, Baseline comparison 7.62-45.72 m, Test 2	75
A.5	Mobile Test 1, Latitude vs. Longitude, Cluster 2 Data	76

List of Tables

2.1	Vincenty's Formulae Variable Definitions	21
2.2	Parameter Table for Percentage value $p, n = 5$	30
3.1	Javad RTK system	37
3.2	Multiple GPS system	38
3.3	Data Recording Equipment used for Base and Rover	39
3.4	GPRMC String Definition [1]	45
3.5	GPGGA String Definition [1]	46
3.6	GPGSA String Definition [1]	46
4.1	Statistical Mobile Test Results - Multiple GPS System - Full Data Set . . .	63
4.2	Statistical Mobile Test Results - Worst Case GPS Pair - Full Data Set . . .	63
4.3	Statistical Mobile Test Results - Javad RTK System - Full Data Set	66
4.4	Statistical Mobile Test Results - Javad RTK System - Partial Data Set . . .	66

Acknowledgments

Throughout my college career, there have been numerous people to thank for my success and I will personally thank those that have helped me the most.

I would like to thank God, who during the storms of my life, has always been the shelter for my soul.

I would like to thank my parents Howard and Debra Trinklein and sister Alison Trinklein. They were instrumental during my college career. With their help, love, and support, I was able to be one of the few in my family who have graduated college with an advanced degree. I'm especially grateful for my father and sister for helping me with acquiring data for my research.

I would like to thank my advisors Gordon Parker and Jason Blough. Their guidance and mentoring was crucial though the many projects that I endeavored while acquiring my graduate degree. These numerous experiences were invaluable and will excel me through the next stages of my life.

I want to thank Douglas Counts and his family. Doug is a good friend and co-worker and has always been there for me. He allowed me to work my way through college while gaining vast experience in the field of engineering.

My fellow students were also an invaluable asset while I was conduction my research. The discussions with Wie Chen, Wenjia Liu, Jill Blecke, Justin Vanness, and Tyler Schoenherr were always insightful and interesting. I was very grateful for having peers available to discuss research and for the comradery it brings.

Abstract

POST PROCESSING OF MULTIPLE GPS RECEIVERS TO ENHANCE BASELINE ACCURACY

Eddy H. Trinklein

Michigan Technological University, 2011

Advisor: Dr. Gordon G. Parker

Inexpensive, commercial available off-the-shelf (COTS) Global Positioning Receivers (GPS) have typical accuracy of ± 3 meters when augmented by the Wide Areas Augmentation System (WAAS). There exist applications that require position measurements between two moving targets. The focus of this work is to explore the viability of using clusters of COTS GPS receivers for relative position measurements to improve their accuracy. An experimental study was performed using two clusters, each with five GPS receivers, with a fixed distance of 4.5 m between the clusters. Although the relative position was fixed, the entire system of ten GPS receivers was on a mobile platform. Data was recorded while moving the system over a rectangular track with a perimeter distance of 7564 m. The data was post processed and yielded approximately 1 meter accuracy for the relative position vector between the two clusters.

1. Introduction

The Global Positioning System, or GPS, is a world-wide radio navigation system that uses a constellation of satellites to provide accurate positioning, velocity and time to any user with appropriate receiving equipment. Originally developed in the 1960s for military use, it was opened up for civilian use in 1996 and now has millions of users world-wide. GPS satellites continuously transmit specifically coded signals that can be decoded by a user's GPS receiver. The signals are divided into two types, Standard Positioning Service (SPS) for civilian use and Precision Positioning Service (PPS) for U.S. military use [2]-[4].

In this chapter, a brief overview of how GPS works will be presented. The operation segments of GPS will be introduced and will be followed by the principle of GPS operation. An overview of the error sources that are associated with GPS will be developed. Once the error sources are defined, the common methods for increasing GPS accuracy will be discussed. The focus of this thesis is the use of low cost GPS receivers to improve their ability to measure relative positions. This is described in more detail at the end of this chapter.

1.1 GPS Operational Components

The GPS has three components, referred to as "segments", the space segment, the user segment, and the control segment. These are briefly described below.

1.1.1 Space Segment

The space segment consists of a minimum of 24 satellites in orbit around the Earth. At a height of 20,200 km above the surface of the Earth, each satellite has a 12 hour orbital period. While 24 is the nominal number of satellites, generally more are in orbit to allow newer satellites to replace older ones without violating the 24 satellite minimum. The orbits are divided into six planes with at least four satellites per plane. The GPS constellation is shown in Figure 1.1, where the sphere in the center represents the Earth and the inner circle around the sphere is the equatorial plane. Around the sphere, the orbits are shown as the larger circles with the satellites constrained to them. This satellite constellation provides users with a minimum of five satellites visible from any point on Earth at all times.

1.1.2 User Segment

The user segment is made up of millions of GPS receivers world-wide in both the civilian and military sectors. A GPS receiver converts the signals transmitted by the visible satellites into three dimensional position and a Coordinate Universal Time, abbreviated UTC. A minimum of four satellites are required to resolve the four dimensions of X, Y, Z, and time.

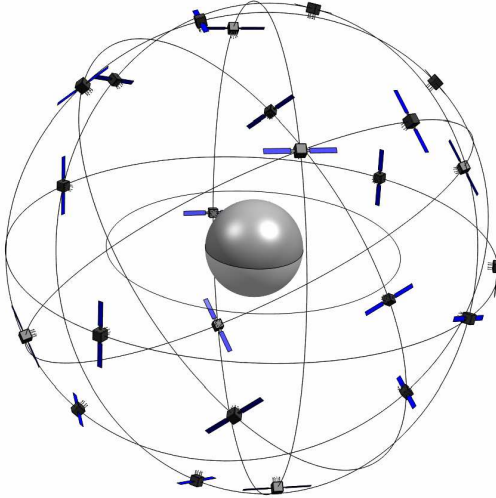


Figure 1.1. GPS Orbits.

Navigation is the primary function of GPS receivers, and is used by ships, aircraft, ground vehicles and individuals. It should be noted that the satellites only transmit, therefore an infinite number of users are possible.

1.1.3 Control Segment

The control segment is comprised of five ground based monitoring and tracking stations located at specific locations on the Earth. The control segment is in continuous communication with each GPS satellite, monitoring their health, precise orbits (ephemeris), and on-board clock biases. The GPS master control facility is located in Colorado at the Schriever Air Force Base. Four unmanned monitoring stations are located in Hawaii, Ascension Island, Diego Garcia, and Kwajalein; all of which are near the equator [3],[5].

1.2 GPS Satellite signals

GPS satellites transmit two microwave carrier signals, the L1 frequency (1575.42 MHz) and the L2 frequency (1227.60 MHz). The carrier signals are phase-modulated by three Pseudo Random Noise (PRN) codes used for position calculation. The PRN codes, while described as random are actually mathematically determinant and can be replicated by GPS receivers. Carrier signal L1 is modulated by the Course Acquisition code (C/A), a 1.023 MHz noise-like code that repeats every 1023 bits or one millisecond. Each satellite has a unique C/A code that it transmits and is used by the civilian SPS. The U.S. Government implemented a more accurate code, Precision Positioning Service (PPS), for use with military personnel or those granted access. This more accurate code is modulated onto the phase of the L1 and L2 carrier signals at 10.23 MHz, is encrypted, and repeats every seven days. Decryption requires a classified module for each channel of the receiver with access granted only by the U.S. Government. A navigation message is also modulated onto the L1 signal and contains 50 Hz updates of satellite orbits, clock corrections, and other parameters [2]-[5].

1.3 The GPS Concept

GPS relies on the basic principle of calculating a position in space relative to several known locations. The unknown location is found by intersecting several spheres by a process called trilateration. To illustrate trilateration, two examples will be presented and then used to develop the equations that determine a user's position.

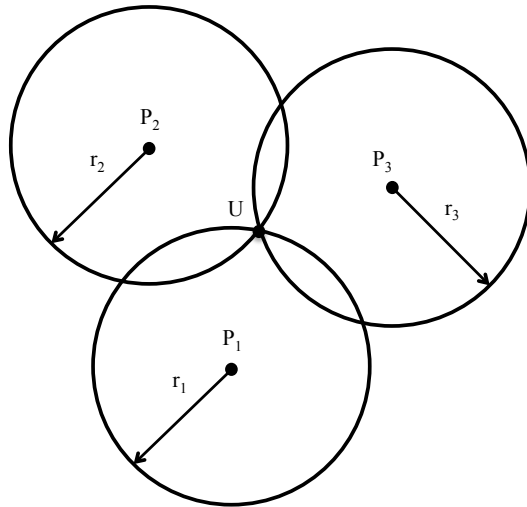


Figure 1.2. Two dimensional user position.

1.3.1 Two Dimensional Case

Consider the two dimensional case shown in Figure 1.2. The points P_1 - P_3 are known positions. The "user" position is at point U , where only its distance relative to P_1 - P_3 is known and denoted r_1 - r_3 . The user position is constrained to an infinite number of possible locations defined by the circle with origin at P_1 and radius r_1 . If there is a second known location, P_2 , and the distance to the user, r_2 , is known this further constrains the user position to two points, located at the intersection of the two circles. A third known location, P_3 , with distance r_3 , uniquely identifies the user position. Therefore, three known locations and three distances are required to resolve user position in this two dimensional case.

1.3.2 Three Dimensional Case

Now Consider the three dimensional case shown in Figure 1.3. In the Figure, x , y , and z represent an Earth-Centered Earth-Fixed (ECEF) coordinate system.

This ECEF coordinate system is fixed to the center of mass of the Earth where $+x$ points in the direction of 0° longitude, $+y$ points toward 90° E longitude, and $+z$ points toward north, normal to the equatorial plane. Latitude denoted ϕ , is defined as the angle between the x - y plane and any vector from the origin to a point on the surface of the Earth where positive ϕ is about the x -axis. This coordinate system is convenient for calculating a user position on the surface of the Earth. In three dimensions, spheres replace the circles used conceptually in two dimensions. The known location P_1 has known coordinates (x_i, y_i, z_i) . The distance from P_i to U is denoted r_i . If there is only one known position P_1 and the distance r_1 from P_1 to U , then an infinite number of possible user positions exist and form a sphere. If there is a second known position, P_2 , and known distance to the user, r_2 , a second sphere is formed. The intersection of these two spheres constrains the possible solution space to a circle. The third known location, P_3 , and user distance, r_3 , form a third sphere that intersects the other, reducing the possible solutions down to two. Given that the user will be on or near the surface of the Earth, the ambiguity between the two solutions can be resolved since one solution will be near the surface of the Earth and the other will be far from it.

Similar to two dimensions, three locations are required to uniquely determine a user position for the general three-dimensional case. From Figure 1.3, three simultaneous equations can be derived from the Cartesian representation of a sphere, and are given as Eq. 1.1 [2]-[4], where the location of U is denoted by x_u, y_u, z_u .

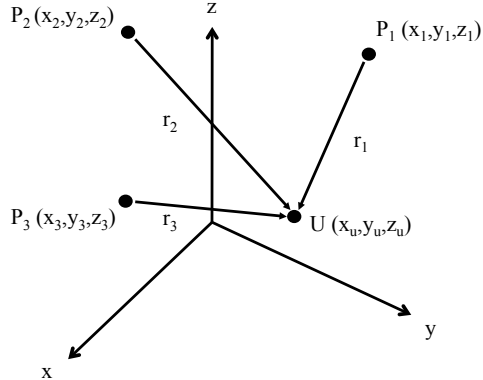


Figure 1.3. Three dimensional user position.

$$\begin{aligned}
 r_1 &= \sqrt{(x_1 - x_u)^2 + (y_1 - y_u)^2 + (z_1 - z_u)^2} \\
 r_2 &= \sqrt{(x_2 - x_u)^2 + (y_2 - y_u)^2 + (z_2 - z_u)^2} \\
 r_3 &= \sqrt{(x_3 - x_u)^2 + (y_3 - y_u)^2 + (z_3 - z_u)^2}
 \end{aligned} \tag{1.1}$$

If the three positions x_i, y_i, z_i and the spherical radii $r_i, i = 1..3$ are known, then the user position, x_u, y_u, z_u , can be determined, by solving three nonlinear coupled equations. For the GPS application the P_i are the known satellite locations and the r_i are their reported distances to the receivers. The r_i will now be called pseudoranges to imply expected errors which are described in Section 1.4.

A GPS receiver position is calculated using satellite pseudoranges and positions data at each broadcast time, referred to as an epoch. To obtain this pseudorange, the satellites continuously transmit C/A code, which contains satellite ephemeris data, time, correction factors, almanac, and satellite health status. Each satellite transmits its own unique C/A code and is exactly reproduced by the receiver. Each C/A code that is received, is time

shifted to match the receiver generated code. This time shift, corresponds to a distance which defines the radius of the satellite sphere to which the user is constrained or the r_i of the earlier examples. The C/A code is transmitted as electromagnetic energy traveling at the speed of light, or approximately $c \approx 299,792,458$ m/s. The true range between the receiver and the i^{th} satellite, ρ_{iT} , can be estimated using Eq. 1.2,

$$\rho_{iT} = c(t_u - t_{si}) \quad (1.2)$$

where t_u is the true reception time and t_{si} is the i^{th} satellite time.

Of the known sources of error in GPS, which will be further investigated in Section 1.4, the receiver clock bias can be directly corrected by augmenting Eq. 1.1 with a receiver clock bias term, b_u . Adding this bias term requires another satellite to solve for the additional unknown, resulting in Eq. 1.3,

$$\begin{aligned}\rho_1 &= \sqrt{(x_1 - x_u)^2 + (y_1 - y_u)^2 + (z_1 - z_u)^2} + b_u \\ \rho_2 &= \sqrt{(x_2 - x_u)^2 + (y_2 - y_u)^2 + (z_2 - z_u)^2} + b_u \\ \rho_3 &= \sqrt{(x_3 - x_u)^2 + (y_3 - y_u)^2 + (z_3 - z_u)^2} + b_u \\ \rho_4 &= \sqrt{(x_4 - x_u)^2 + (y_4 - y_u)^2 + (z_4 - z_u)^2} + b_u\end{aligned} \quad (1.3)$$

It should be noted that b_u has units of distance. It is related to the bias time, t_b by $b_u = c t_b$.

1.4 GPS Error Sources

There are several sources of error in where using GPS for determining receiver positions. These errors can be categorized into six different types; clock errors, receiver noise, ephemeris errors, atmospheric effects, multipath interference and electrical interference.

1.4.1 Clock Errors

Satellite or receiver clock biases can result in very large positioning errors. For example, an error of only one microsecond results in a $c/10^6 = 300$ m position error. Each satellite contains at least one, high accuracy (10^{-9} s/day), atomic clock. Atomic clocks, while accurate, are very expensive and therefore quartz clocks are typically used in receivers and have an accuracy of about 0.5 s/day. Fortunately for users, the clock bias can be removed during the pseudorange calculation, as described in Section 1.3.2.

1.4.2 Receiver Noise

Inexpensive GPS receivers are susceptible to different types of noise. Thermally induced noise is caused by the random motion of electrons in electrical conductors operating above absolute zero (0 K) [6]. A GPS receiver's antenna is effected by radiation energy emitted from the ground, sky and near by objects. This is because all objects above 0 K emit radiation energy, which can cause errors in the pseudorange measurements of 1.5 meters [7]. Errors are also introduced due to part-to-part manufacturing differences of the receivers.

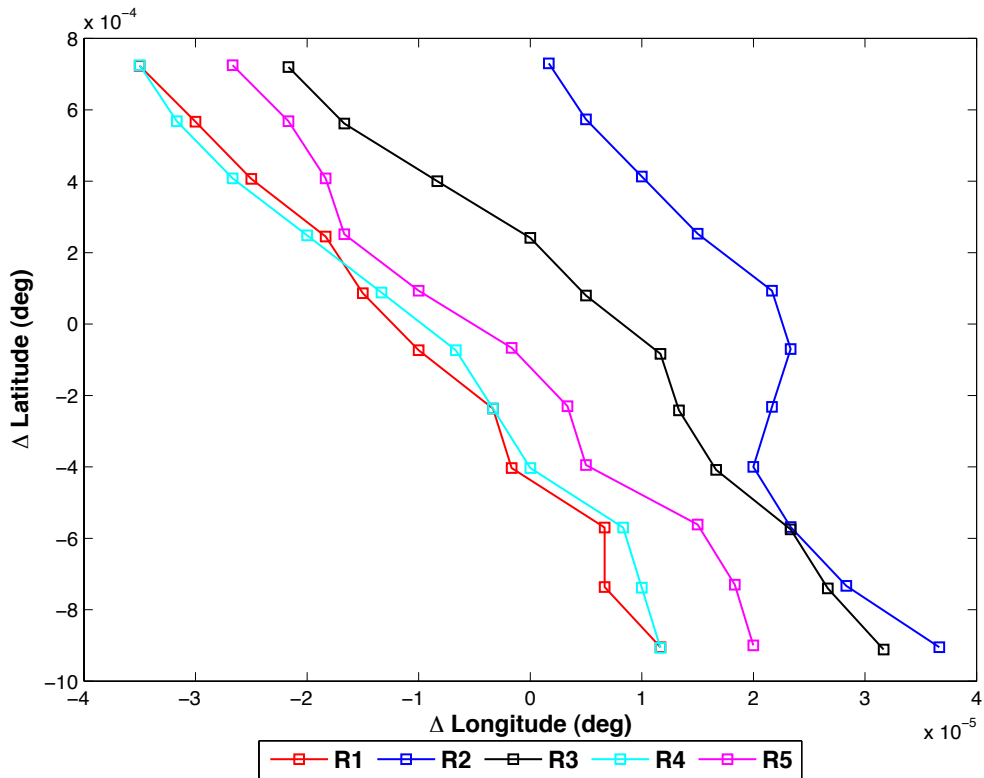


Figure 1.4. Mobile Data comparing Raw Latitudes vs. Longitudes.

The electronic components used are not identical, resulting in slightly different positioning solutions receiver to receiver. This fact is shown in Figure 1.4, where ten seconds of raw latitude vs. longitude data is shown from five identical receivers. Although they are only a few centimeters apart and below their distance measurement noise floor, the recorded differences in position are up to a few meters apart. This behavior also occurs using stationary data. Mathematical rounding and quantization level which determines the noise floor also cause receiver noise.

1.4.3 Ephemeris Errors

The satellite positioning error, or ephemeris errors, are differences in the reported satellite position and actual position at a given epoch. While the position of each satellite is continuously tracked and updated, some error will always be present. Referring back to the introduction examples, ephemeris errors are errors in the known locations, P_i . Along with the actual positions of the satellites, the orientation of the satellites relative to each other is also important. If the satellites visible by the receiver are grouped close together, the accuracy of the estimated receiver position will decrease as compared to when the satellites are relatively far apart.

1.4.4 Atmospheric Effects

The Ionosphere, an electrically charged part of the atmosphere, acts like a mirror and bends the satellite signal, resulting in a time delay error. A dual frequency receiver can directly correct the effects of the Ionosphere by determining the difference in the propagation of the two frequencies. Dual frequency antennas are typically found only on expensive GPS receivers. For single frequency receivers, an Ionosphere model is built into the receiver to model this error and to correct for the time delay. The Troposphere causes similar refractive effects mainly due to water vapor and weather. Thus day-to-day weather changes will cause a stationary receiver position measurement to vary.

1.4.5 Multipath Interference

Multipath interference occurs when the satellite signal is reflected off objects near the receiver. This reflection is another source of time delay error. In some cases, such as in large cities with tall buildings, the multipath effects can be significant. Also in large cities, the number of satellites in view can be reduced due to shading effects caused by buildings or other objects in the line of sight.

1.4.6 Electrical Interference

Electrical interference can be of two types, intensional and unintentional. Intensional, or GPS jamming can reduce the accuracy or completely prevent a receiver to lock onto satellites. Jamming devices introduce noise onto the $L1$ and $L2$ carrier signals that effectively blocks the incoming signals. Unintentional electrical interference can come from anything that produces electrical frequencies near the $L1$ and $L2$ frequencies. These devices can be computers, cell phones, and radio equipment. Electrical interference is not typically modeled, but is included here as a possible source for errors.

1.4.7 GPS Error Summary

Reference [2] encompasses the biasing errors as shown in Eq. 1.4,

$$\rho_i = \rho_{iT} + \Delta D_i - c(\Delta b_i - b_{ut}) + c(\Delta T_i + \Delta I_i + v_i + \Delta v_i) \quad (1.4)$$

where ρ_i is the measured pseudorange, ρ_{iT} is the true pseudorange, ΔD_i is the satellite positioning error effect on range, Δb_i is the satellite clock error, b_{ut} is the receiver clock bias, ΔT_i is Tropospheric delay error, ΔI_i is the ionospheric delay error, v_i is receiver measurement noise, and Δv_i is the relativistic time correction.

1.5 GPS accuracy

1.5.1 Standard Positioning Service accuracy

Standard Positioning Service (SPS) accuracy was originally designed with Selective Availability (SA), which limited the accuracy to 100 meters for the civilian sector. SA adds intentional time errors to the satellite pseudoranges to increase the error in resolved position. On May 1, 2000, SA was turned off and SPS accuracy increased to 20 meters. For most GPS users this accuracy is sufficient, but enhancements have been developed to further increase the performance of GPS, which usually results in increased receiver cost. Two types of GPS enhancements are Differential GPS (DGPS) and Real Time Kinematic (RTK) GPS.

1.5.2 Differential GPS accuracy

Differential GPS (DGPS) is an enhancement that uses a network of GPS receivers at known locations to transmit corrections to mobile GPS receivers. DGPS is designed to correct errors common to each receiver such as ephemeris errors (ΔD_i), atmospheric effects (ΔT_i and ΔI_i), and clock errors (Δb_i and b_{ut}). Typically the corrections are transmitted using UHF radios. Since the correction is passively transmitted, multiple GPS receivers can be corrected simultaneously. The principle of DGPS is that the base station is placed at a known location that is determined before measurements are to be made. The difference between the known location and the reported position is the correction transmitted to the participating receivers, known as rovers. DGPS works best when the base station and the rovers have relatively short distances between them. As the distance increases, the errors between the base and rover units become less correlated and accuracy decreases especially due to atmospheric errors. The accuracy attained using DGPS is 3-5 meters, which occurs 95% of the time, depending on the equipment used and the distance between the base and rovers.

1.5.3 WAAS DGPS accuracy

Another form of DGPS is the Wide Area Augmentation System, or WAAS, which is available in North America. WAAS uses geostationary satellites to transmit corrections to ground receivers. The WAAS satellites are similar to GPS satellites and transmit corrections and also range information, effectively increasing the number of satellites available for position calculation. A network of ground stations collect data from the GPS satellites and calculate a correction that is then broadcast to the WAAS satellites.

The WAAS satellites then send this correction to local ground receivers. The transmitted corrections are in two forms, fast and slow. The fast correction is similar to a normal GPS solution but is enhanced by ground stations corrections. Once the receiver, obtains a corrected solution applied to the next position solution, the slow correction can be applied. The slow correction includes information about the Ionosphere and is updated every two minutes. The slow correction is considered good up to six minutes because Ionosphere delays do not change rapidly. In North America, WAAS correction is free to all GPS users that have WAAS corrected receivers and yields position accuracies of three meters 95% of the time [1].

1.5.4 Real Time Kinematic accuracy

Real Time Kinematic (RTK) GPS is yet another enhancement of GPS yielding centimeter accuracy. This technique is similar to DGPS, where there is a base station at a known location and a rover with unknown coordinates. The increase in accuracy comes from using the carrier phase for determining the position rather than the information encoded onto the carrier signal. For the L1 carrier signal, the accuracy based on its wavelength of 19.0 cm and a 1% error in the phase measurement is 1.9 cm, which does not take into account other types of errors. The difficult task in RTK GPS is ensuring that the carrier phase does not “slip”, meaning to gain or lose an integer multiple of the wavelength, adding an error of 19 cm or $n \times 19$ cm. Significant proprietary development has been invested by companies marketing RTK GPS and thus commercially available devices are expensive compared to non-RTK GPS receivers.

1.5.5 Post Processing Techniques

Post processing receiver data can increase GPS accuracy with varying levels of implementation difficulty and cost. A form of offline DGPS as described in Section 1.5.2, can be used to correct a saved data set by shifting the data relative to a known location, such as a survey marker. This requires knowing the location used to correct the data set with a high level of accuracy. There are also internet based services that will post process a data set with corrections that are calculated from multiple fixed GPS receivers. In this thesis, a post processing technique was developed that uses the coordinates recorded from two clusters of multiple GPS receivers to increase the measurement accuracy of the distance between them.

1.6 Proposed Post Processing Algorithm

A post processing algorithm was developed to increase the accuracy of the distance measurement between two clusters of inexpensive GPS receivers as shown in Figure 1.5.

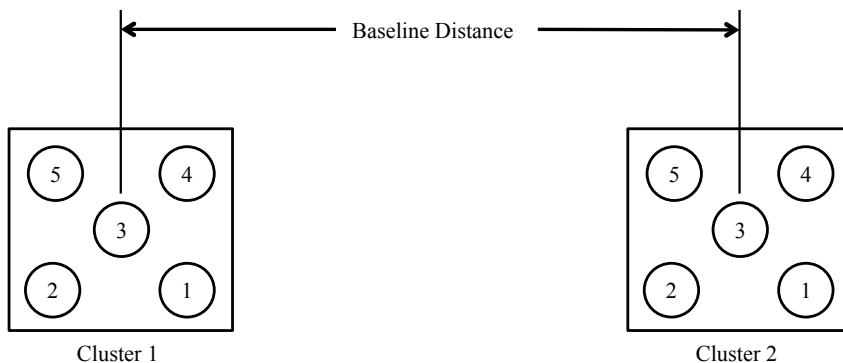


Figure 1.5. Baseline Distance between Two GPS Clusters.

The distance between the central receiver of each clusters will be called the baseline distance. In this application, the setup is similar to DGPS. The difference is using two *clusters* of receivers as compared to using only two receivers to form a DGPS setup. Therefore, all the benefits of DGPS are fully realized, such as correcting for ephemeris, atmospheric, and clock errors. However, as shown in Figure 1.4, the receiver noise is not corrected using only two receivers to obtain DGPS. Therefore, a post processing algorithm was developed that uses an efficient approach to increase baseline distance accuracy by reducing receiver noise. The algorithm is efficient in that the averaging and filtering techniques are simple to implement, execute quickly, and the hardware used is inexpensive. A particular focus of this work was to explore differences between stationary and mobile applications of this approach.

As with many things in life, price and performance typically both trend upwards. The question becomes how much performance is required for a set price range? And if a certain performance is required, the price may be higher than what the consumer is willing to pay. In this thesis, the performance, or accuracy more specifically, is compared between two GPS systems. The first is an expensive and highly accurate Javad RTK GPS system and the second is the multiple GPS system described above.

The post processing algorithm first performs a truncated mean averaging algorithm to integrate the multiple GPS coordinates of each cluster into a single set of latitudes and longitudes. A moving average filter was then applied to the averaged latitudes and longitudes to remove random variations. The baseline distance between the two clusters was calculated using Vincenty's Formulae [8]. The baseline distances under investigation were less than 100 meters. The altitude difference between the two clusters was not considered and all testing was conducted on relatively level ground.

The algorithm was investigated for stationary and the main application of this thesis, mobile applications, such as a towed vehicle or coordinated motion of two objects.

The idea of using multiple receivers to increase GPS accuracy, determine attitude, or to enhance Inertial Measurement Unit (IMU) performance was explored in the 1990's and early 2000's as discussed in references [9]-[13]. These past efforts all use the multiple GPS receiver concept to increase the performance of a navigation solution. However, their implementation requires intricate knowledge of the low level operation of the specific GPS receiver used. The focus of this effort was on commercial off the shelf GPS receivers without access to their proprietary operational details.

2. Post Processing Algorithm

In this chapter, the post processing technique will be explained. Vincenty's formulae, used for the calculating distance between two points, will be described. A coordinate translation that could be used to shift the GPS latitudes and longitudes within a cluster to a single point will be explained. The method of averaging the individual GPS coordinates into a single set of latitudes and longitudes will be discussed. The filtering technique used to smooth the averaged coordinates is presented. The combination of these subsystems defines the post processing algorithm.

2.1 Vincenty's Formulae for Determining Distance Between Two Points

Calculating the distance between two locations is not a trivial task. The method used in this thesis to calculate the baseline distance is Vincenty's formulae [8]. There are two forms of Vincenty's formulae and are iterative methods for determining the distance between two locations on the Earth. The first method (direct) calculates the location of a point given an azimuth, which is a direction relative to north, and the distance from a known location.

The second method (inverse) calculates the azimuth and the baseline distance between the two points along the surface of the Earth, known as geographical distance. The formulae are accurate to 0.5 mm and are commonly used in geodesy, a form of earth sciences focused on representation and measurement of the Earth. The high accuracy is due to modeling the Earth as an oblate spheroid, which takes into account the flattening of the Earth near the north and south poles. Vincenty's formulae are more accurate than spherical approximations of the Earth as in the great-circle distance method. Vincenty's formulae are complex and require longer computation times to reach a solution as compared to great-circle distance methods. Both Vincenty's formulae and great circle distance methods do not take into account altitude. A table of variable definitions used in both the direct and inverse methods is shown in Table 2.1. The direct and indirect method formulas are given as Equation 2.1 through 2.16 and Equation 2.8 through 2.31 respectively [8]. The variable definitions provided in Table 2.1 are evaluated initially and are applicable for both the direct or inverse methods. The constants a , b , and f are defined by the World Geodetic System WSG 84 model and define the oblate spheroid Earth model. The constants a , b , and f are nominally 6,378,137.0 meters, 6,356,752.314 meters, and 1/298.257223563 respectively.

2.1.1 Vincenty's Direct Method

The direct method calculates the latitude and longitude location of an end point (ϕ_2, λ_2) given an initial point latitude and longitude (ϕ_1, λ_1) , an initial azimuth (α_1) , and a distance, s , along the surface of the oblate spheroid model of the Earth. The direct method is executed using three steps. Step one is to evaluate Equations 2.1 through 2.7.

Table 2.1.
Vincenty's Formulae Variable Definitions

Variable	Definition
a	length of major axis of the ellipsoid (radius at the equator)
b	length of minor axis of the ellipsoid (radius at the poles)
$f = (a - b)/a$	flattening of the ellipsoid
ϕ_1, ϕ_2	latitude of the points
$U_1 = \arctan[(1 - f)\tan\phi_1]$	reduced latitude
$U_2 = \arctan[(1 - f)\tan\phi_2]$	reduced latitude
λ_1, λ_2	longitude of the points
$L = \lambda_2 - \lambda_1$	difference in longitudes
α_1, α_2	forward and reverse azimuths
α	azimuth at the equator
s	ellipsoidal distance between the two points

$$\tan U_1 = (1 - f) \tan \phi_1 \quad (2.1)$$

$$\sigma = \arctan\left(\frac{\tan U_1}{\cos \alpha_1}\right) \quad (2.2)$$

$$\sin \alpha = \cos U_1 \sin \alpha_1 \quad (2.3)$$

$$\cos^2 \alpha = (1 - \sin \alpha)(1 + \sin \alpha) \quad (2.4)$$

$$u^2 = \cos^2 \alpha \frac{a^2 - b^2}{b^2} \quad (2.5)$$

$$A = 1 + \frac{u^2}{16384} \left\{ 4096 + u^2 \left[-768 + u^2 (320 - 175u^2) \right] \right\} \quad (2.6)$$

$$B = \frac{u^2}{1024} \left\{ 256 + u^2 \left[-128 + u^2 (74 - 47u^2) \right] \right\} \quad (2.7)$$

Step two is to iterate Equations 2.8 through 2.10, using an initial value of $\sigma = \frac{s}{bA}$, until σ does not significantly change.

$$2\sigma_m = 2\sigma_1 + \sigma \quad (2.8)$$

$$\Delta\sigma = B \sin \sigma \left\{ \cos(2\sigma_m) + \frac{1}{4}B \left[\cos \sigma (-1 + 2 \cos^2(2\sigma_m)) \right. \right. \\ \left. \left. - \frac{1}{6}B \cos(2\sigma_m)(-3 + 4 \sin^2 \sigma)(-3 + 4 \cos^2(2\sigma_m)) \right] \right\} \quad (2.9)$$

$$\sigma = \frac{s}{bA} + \Delta\sigma \quad (2.10)$$

Step three is to evaluate Equations 2.11 through 2.16 to obtain the coordinates of the end point and the reverse azimuth, α_2 .

$$\phi_2 = \arctan \left(\frac{\sin U_1 \cos \sigma + \cos U_1 \sin \sigma \cos \alpha_1}{(1-f)\sqrt{\sin^2 \alpha + (\sin U_1 \sin \sigma - \cos U_1 \cos \sigma \cos \alpha_1)^2}} \right) \quad (2.11)$$

$$\lambda = \arctan \left(\frac{\sin \sigma \sin \alpha_1}{\cos U_1 \cos \sigma - \sin U_1 \sin \sigma \cos \alpha_1} \right) \quad (2.12)$$

$$C = \frac{f}{16} \cos^2 \alpha [4 + f(4 - 3 \cos^2 \alpha)] \quad (2.13)$$

$$L = \lambda - (1-C)f \sin \alpha \left\{ \sigma + C \sin \sigma [\cos(2\sigma_m) \right. \quad (2.14)$$

$$\left. + C \cos \sigma (-1 + 2 \cos^2(2\sigma_m)) \right\} \quad (2.15)$$

$$\alpha_2 = \arctan \left(\frac{\sin \alpha}{-\sin U_1 \sin \sigma + \cos U_1 \cos \sigma \cos \alpha_1} \right) \quad (2.16)$$

2.1.2 Vincenty's Inverse Method

The inverse method calculates the distance between two points, s , and forward and reverse azimuths (α_1, α_2) given the coordinates (ϕ_1, λ_1) and (ϕ_2, λ_2) . The inverse method is executed using two steps. The first step is to calculate U_1, U_2, L , set $\lambda = L$ as an initial value, and then iterate Equations 2.17 through 2.24 until λ converges. If the two points are nearly antipodal, meaning the points are diametrically opposed and on opposite sides of the Earth, λ may fail to converge.

$$\sin \sigma = \sqrt{(\cos U_2 \sin \lambda)^2 + (\cos U_1 \sin U_2 - \sin U_1 \cos U_2 \cos \lambda)^2} \quad (2.17)$$

$$\cos \sigma = \sin U_1 \sin U_2 + \cos U_1 \cos U_2 \cos \lambda \quad (2.18)$$

$$\sigma = \arctan \frac{\sin \sigma}{\cos \sigma} \quad (2.19)$$

$$\sin \alpha = \frac{\cos U_1 \cos U_2 \sin \lambda}{\sin \sigma} \quad (2.20)$$

$$\cos^2 \alpha = 1 - \sin^2 \alpha \quad (2.21)$$

$$\cos(2\sigma_m) = \cos \sigma - \frac{2 \sin U_1 \sin U_2}{\cos^2 \alpha} \quad (2.22)$$

$$C = \frac{f}{16} \cos^2 \alpha [4 + f(4 - 3 \cos^2 \alpha)] \quad (2.23)$$

$$\begin{aligned} \lambda = L + (1 - C) f \sin \alpha & \left\{ \sigma + C \sin \sigma [\cos(2\sigma_m) \right. \\ & \left. + C \cos \sigma (-1 + 2 \cos^2(2\sigma_m))] \right\} \end{aligned} \quad (2.24)$$

Once λ has converged to a small number (10^{-12}), Equations 2.25 through 2.31 are evaluated to determine the distance between the points, s , and the forward and reverse azimuths (α_1, α_2) .

$$u^2 = \cos^2 \alpha \frac{a^2 - b^2}{b^2} \quad (2.25)$$

$$A = 1 + \frac{u^2}{16384} \left\{ 4096 + u^2 \left[-768 + u^2 (320 - 175u^2) \right] \right\} \quad (2.26)$$

$$B = \frac{u^2}{1024} \left\{ 256 + u^2 \left[-128 + u^2 (74 - 47u^2) \right] \right\} \quad (2.27)$$

$$\begin{aligned} \Delta\sigma = B \sin \sigma & \left\{ \cos(2\sigma_m) + \frac{1}{4} B \left[\cos \sigma (-1 + 2 \cos^2(2\sigma_m)) \right. \right. \\ & \left. \left. - \frac{1}{6} B \cos(2\sigma_m) (-3 + 4 \sin^2 \sigma) (-3 + 4 \cos^2(2\sigma_m)) \right] \right\} \end{aligned} \quad (2.28)$$

$$s = bA(\sigma - \Delta\sigma) \quad (2.29)$$

$$\alpha_1 = \arctan \left(\frac{\cos U_2 \sin \lambda}{\cos U_1 \sin U_2 - \sin U_1 \cos U_2 \cos \lambda} \right) \quad (2.30)$$

$$\alpha_2 = \arctan \left(\frac{\cos U_1 \sin \lambda}{-\sin U_1 \cos U_2 + \cos U_1 \sin U_2 \cos \lambda} \right) \quad (2.31)$$

2.2 Receiver Coordinate Translation

The first step in using multiple GPS receivers is to shift the latitudes and longitudes of all the receivers in a cluster to a single reference point. For example, if two receivers are mounted to a rigid base, their location relative to the base-fixed coordinate system can be measured very accurately (sub-millimeter). The latitudes and longitudes generated by each receiver can then be shifted to any point in the base fixed frame. However, if the dimensions between the receivers are below the noise floor of the particular receiver, the all the receivers in the cluster can be considered as the same point. This will introduce a small but quantifiable error, whose importance depends on the baseline distance.

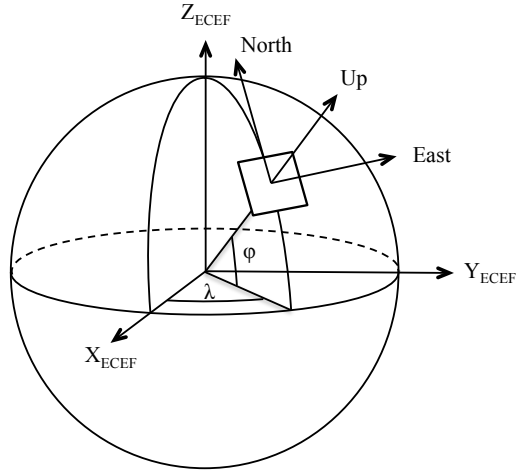


Figure 2.1. ECEF and ENU Coordinate System Relationship

For example, if the maximum distance between the two receivers in the cluster is 0.1 meters and the distance between the clusters is 10 meters, the maximum error introduced by assuming all receivers in the cluster are co-located is $0.1/10 \cdot 100\% = 1\%$. If the receiver separation distance is large compared to the baseline distance then translating the receiver measurements to a single reference point is advised.

One method to perform the coordinate translation is explained for the sake completeness, however was not applied in further analysis. To develop the translation, the relationship between the Earth-Centered Earth-Fixed coordinate system, as developed in Section 1.3.2, and the East-North-Up (ENU) Cartesian coordinate system must be established. The ENU coordinate system captures our conventional notion of east, north, and up. The ENU system is related to the ECEF system shown in Figure 2.1. Working in the ENU coordinate system, the receiver coordinate translation is reduced to a two dimensional problem since altitude difference between the receivers is negligible.

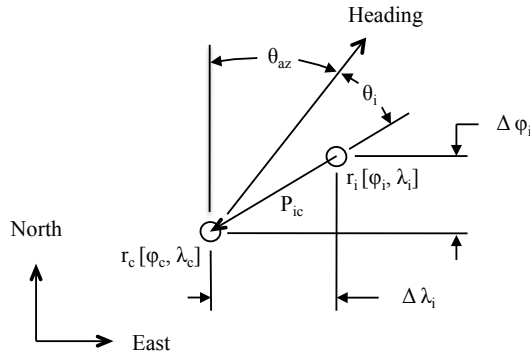


Figure 2.2. Coordinate Translation of a Single Receiver

A single case example of the receiver coordinate translation is shown in Figure 2.2 where r_c represents the central receiver to which the coordinates of a non-central receiver, r_i , are translated to. The radial distance between r_c and r_i is denoted as P_{ic} . The angle θ_{az} is the heading direction of a GPS cluster relative to North, referred to as azimuth and defines the heading direction. The angle θ_i is a constant, which allows for the correction of receivers that are not aligned with the azimuth direction. The two quantities $\Delta\phi_i$ and $\Delta\lambda_i$, are the amount to translate the coordinates of receiver r_i in degrees of latitude and longitude respectively. Since both points r_c and r_i are directly measured in degrees of latitude and longitude (ϕ, λ), the translation is applied to coordinates of receiver r_i . This presents a problem since the distance between the two receivers, P_{ic} , is a measurement in meters, nominally 0.127 meters for the radial distance between receivers in each cluster used in this thesis. This requires P_{ic} to be converted to degrees of latitude and longitude. The conversion is a nonlinear relationship because the Earth is modeled as an oblate spheroid and is dependent on summation of θ_{az} and θ_i . For example, if θ_{az} and θ_i both equal 0° , requiring only a latitude translation, 0.127 meters, is equal to $1.146e^{-6}^\circ$ latitude. Vincenty's direct method was used to determine the conversion based on the distance, azimuth, and an initial point set to $\phi_1 = 43.00^\circ$, $\lambda_1 = -83.00^\circ$, selected near the testing site.

Alternately, if θ_{az} equals 90° and θ_i equals 0° , only a longitude translation is required, 0.127 meters equals $1.561e^{-6^\circ}$ longitude. Since the Earth is modeled as an oblate spheroid, which in two dimensions is an ellipse, the nonlinear relationship can be described using a modified version of the equations of an ellipse in polar coordinates, given as Equation 2.32. In Equation 2.32, $\Delta\phi_i$ and $\Delta\lambda_i$ are the translation amounts in latitude and longitude. The two constants, as described above, $P_{\phi_i} = 1.146e^{-6^\circ}$ and $P_{\lambda_i} = 1.561e^{-6^\circ}$ are the ellipse quadrant values in degrees. The translation is applied to non-central receivers using Equation 2.33, where ϕ_{t_i} and λ_{t_i} are the translated coordinates.

$$\begin{aligned}\Delta\phi_i &= P_{\phi_i} \cos(\theta_{az} + \theta_i) \\ \Delta\lambda_i &= P_{\lambda_i} \sin(\theta_{az} + \theta_i)\end{aligned}\tag{2.32}$$

$$\begin{aligned}\phi_{t_i} &= \phi_i - \Delta\phi_i \\ \lambda_{t_i} &= \lambda_i - \Delta\lambda_i\end{aligned}\tag{2.33}$$

To ensure the proposed translation algorithm was functioning properly, Vincenty's inverse method was used to check the output from Equation 2.33. The inverse method calculates the distance between two points using latitudes and longitudes. The initial point was selected to be 43.00° latitude and -83.00° longitude, the same as used in the direct method examples above.

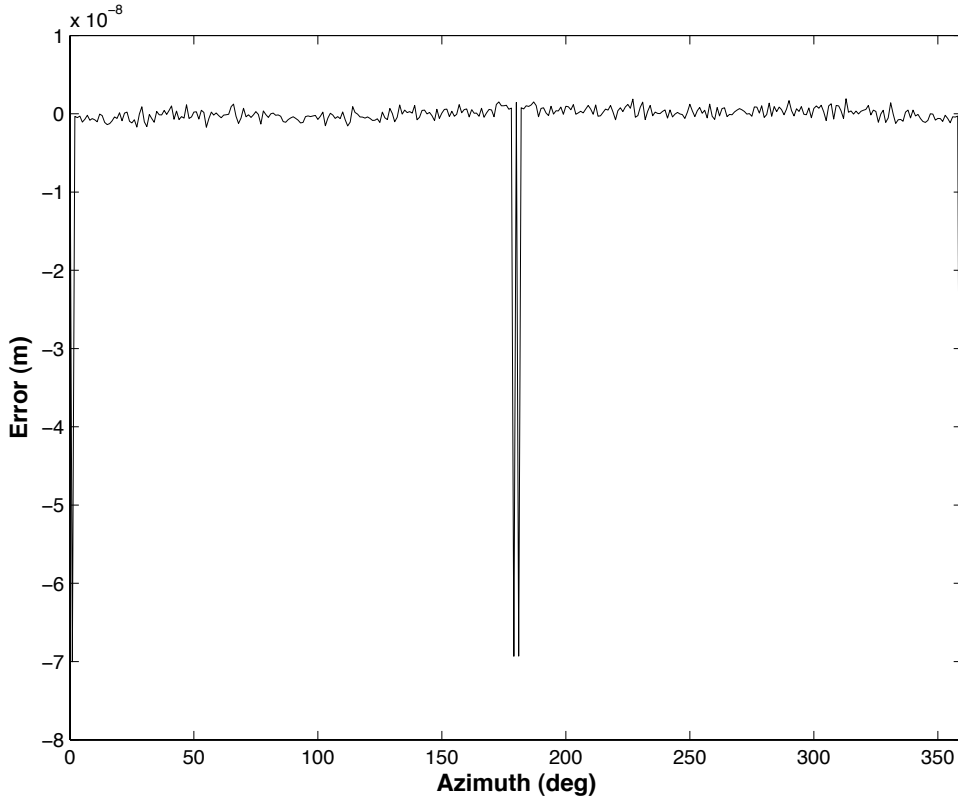


Figure 2.3. Translation Algorithm Error as a Function of Azimuth, Distance 0.127 meters

The final point is the result of Equation 2.33, where the azimuth, θ_{az} was varied from 0 to 360° . The angle θ_i does not effect the resulting distance, it effectively only shifts the azimuth angle on the x axis. The y axis shows the error of the calculated distance, which is well below the measurement tolerance between the receivers. The error appears to be random noise with spikes near 0° and 180° , caused by a singularities or trigonometric sensitivities near these points.

The next step is to obtain the azimuth for the two GPS clusters. One approach is to use Vincenty's inverse method to calculate the azimuth based on the coordinates from the two central receivers (receiver number three) in each cluster, as shown in Figure 2.4.

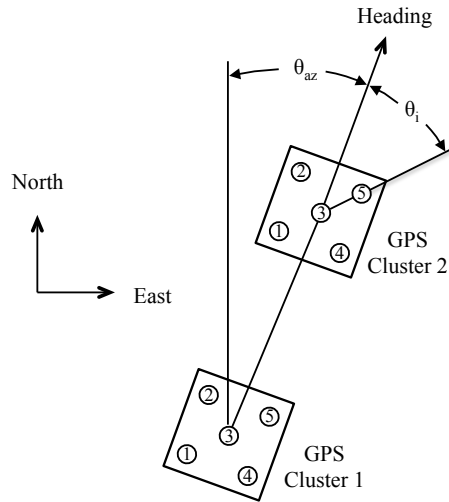


Figure 2.4. Determining Azimuth between two GPS Clusters

This method would work only if the orientation of the clusters is fixed relative to each other during each test. The fixed orientation allows for θ_i to be calculated for each peripheral GPS receiver relative to θ_{az} . If the orientations were not fixed, the resulting translation could result in a large positioning error for the entire cluster. Another method would be to use an orientation sensor to calculate the azimuth directly for each cluster.

2.3 Truncated Mean

In the application of combining the data from several GPS receivers, a truncated mean was selected to average the latitudes and longitudes. A truncated mean is an efficient way of handling outliers in a data set [14]. It works by sorting the data set in ascending order, excluding the highest and lowest k data values, and then computing the mean of the truncated data set, as given as Equation 2.34.

$$k = \left(\frac{n}{2}\right)\left(\frac{p}{100}\right) \quad (2.34)$$

The number of excluded data values depends on the number of data set size, n , and the integer percent value, p . In this thesis, $n = 5$, is the number of GPS receivers used for each cluster. Based on Equation 2.34, it is possible for k to be a non-integer value. This is handled by rounding to the nearest integer value. Typical values of p are between 5 and 25% for larger sample sizes. Since the sample size is only five data points, requiring a higher value for percentage. The resulting number of data points to be averaged is summarized in Table 2.2

In Table 2.2, there are three distinct behaviors of the truncated mean algorithm. When p is selected in the range 1 – 20, all of the data is used for the mean, which would include outliers. The second range of p , 21 – 60, results in throwing out two of the values and averaging the middle three values. The middle setting will reject upper and lower outliers and average the central values. The third range for p , 61 – 99, excludes all data values except the median value. It was decided to use p in the second range, 21 – 60.

Table 2.2.
Parameter Table for Percentage value p , $n = 5$

Percent, p	Data Points Excluded, k	Data Points Averaged
1 - 20	0	5
21 - 60	1	3
61 - 99	2	1

2.4 Moving Average Filtering

In an effort to increase the accuracy of calculated baseline, a filtering technique could reduce the random variations of a data set. In this thesis, the moving average (MA) filter was selected as the filtering scheme applied to the averaged latitudes and longitudes. The MA filter was selected because it works efficiently on time domain data, in this case latitudes and longitudes and executes quickly [15]. The filter weighs all participating data points equally, therefore smoothing out short term fluctuations. The MA filter works similar to a low pass filter that removes high frequency noise. The frequency response of the MA filter is shown in Figure 2.5 as a function of the number of data points that are averaged together, referred to as N . As N increases, the filter becomes more aggressive at attenuating high frequency content. The lobes after the initial filter rolloff provide a smoothing effect in the time domain. The frequency response is plotted up to the Nyquist frequency of π rad/s, corresponding to a one second sampling frequency, which is the update rate of the GPS receivers.

The MA filter is applied using convolution in the time domain. The kernel of the filter is given by Equation 2.35, where x_i is the input data sequence to be filtered.

$$g_{MA} = \frac{1}{N} \sum_{i=0}^N x_i \quad (2.35)$$

During the convolution process, a delay is introduced to the data, which would be a spatial error. To remove this error, the convolution can be applied to the data in both directions of the data, removing the error. Both directions of the data are considered from the first data sample to the end and then from the end of the data to the first sample.

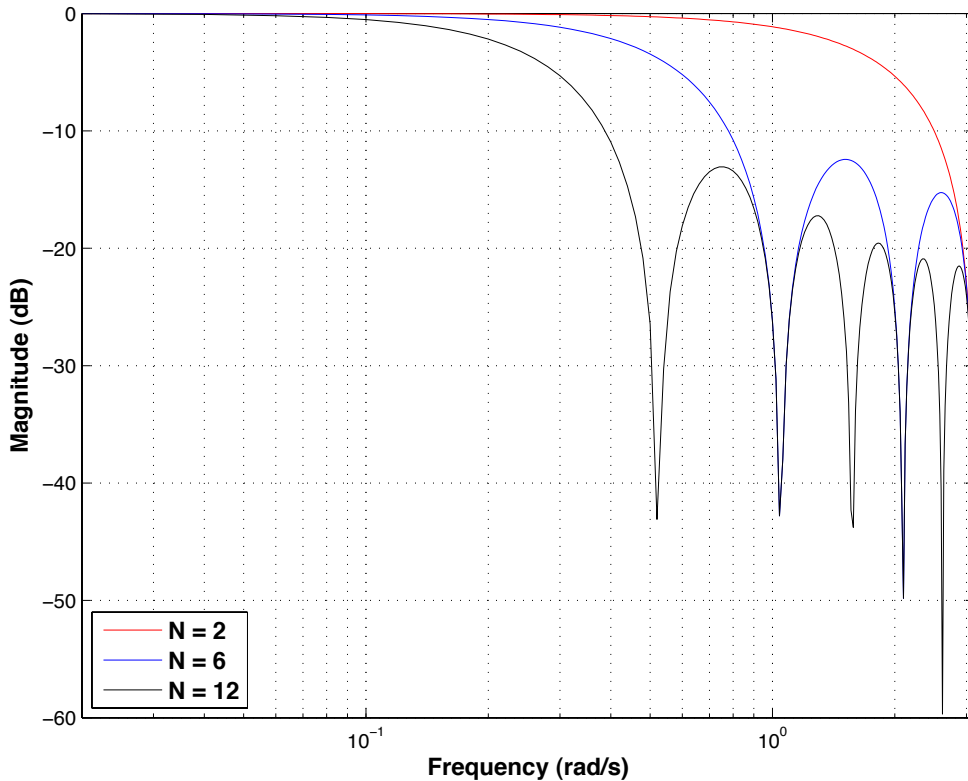


Figure 2.5. Moving Average Filter Frequency Response as a Function of Number of Data Points Used, N

This is also called zero phase shift filtering. In order to select the number of data points to average over, N , preliminary data was captured and processed and is shown as Figures 2.6 and 2.7. This data was collected in a mobile setting, where both clusters were moving together at a 4.48 meter baseline. Details of further testing and results are given in Chapter 4.

In Figure 2.6, the effect of N can be seen on the physical coordinates recorded by the two clusters. As N increases, the low pass filter quality of the MA filter is more pronounced. Using a very accurate GPS system, the Javad RTK, used as the true value for spatial coordinates, the goal was to match the Javad RTK results closely. The MA filter also had a smoothing effect on the baseline distances, which is shown in Figure 2.7.

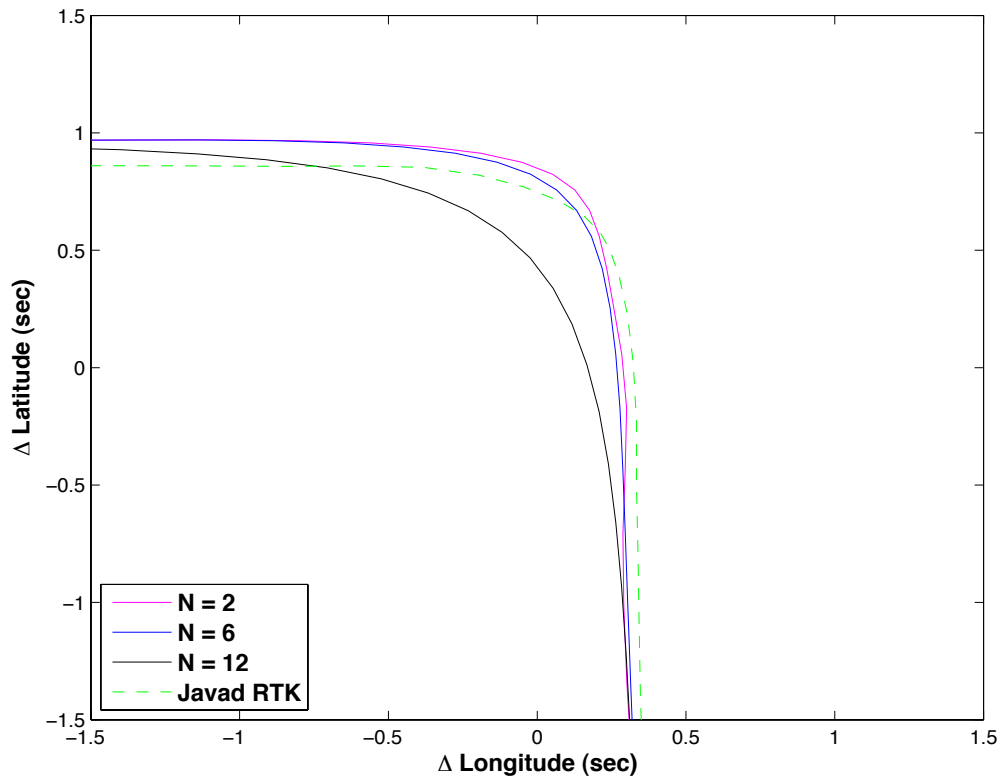


Figure 2.6. Mobile Test 1, 4.48 m Baseline, Effect of Number of Averaged Data Points on Rover Coordinates , Truncated Mean Percent = 50

In Figure 2.7, the effect of N on the calculated baseline can be seen. For low values of N , the high frequency content of the signal is preserved. As N increases, the high frequency content is removed and low frequency trends remain. Based on the preliminary results in Figures 2.6 and 2.7, $N = 6$ was selected for use on all further analysis.

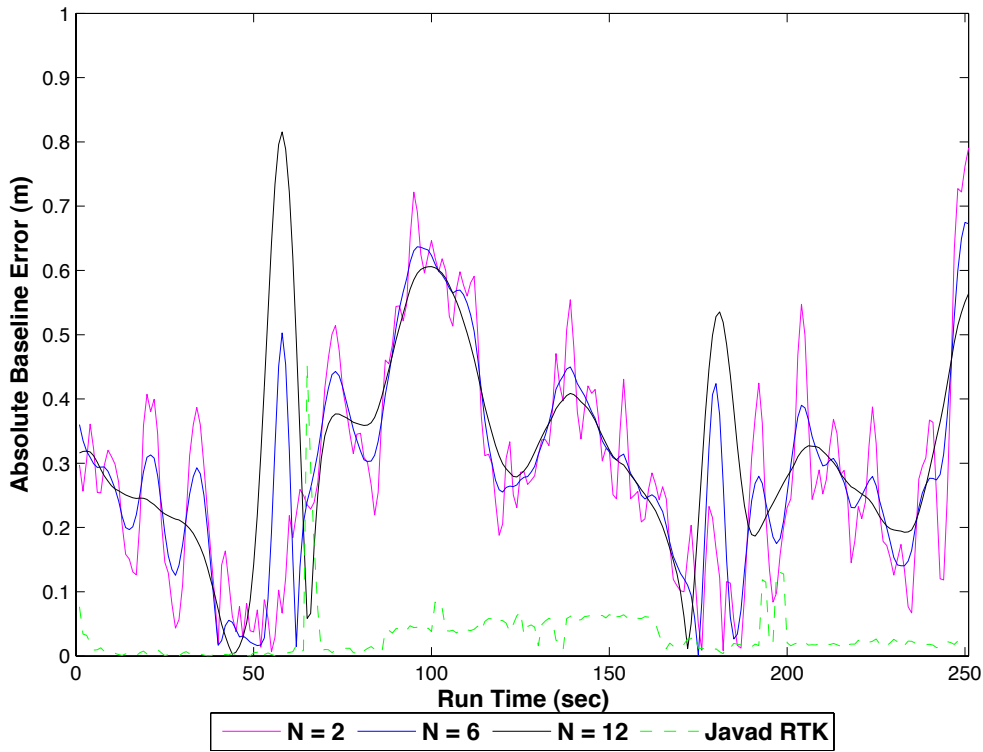


Figure 2.7. Mobile Test 1, 4.48 m Baseline, Effect of Number of Averaged Data Points on Baseline, Truncated Mean Percent = 50

To summarize the post processing algorithm, a flowchart is shown in Figure 2.8. The figure shows how the GPS latitudes and longitudes were manipulated into the final baseline distance. The first step is to record the raw coordinates from the two clusters. Vincenty's inverse method is applied to the coordinates of the central receiver on each cluster to obtain an azimuth. The azimuth is then used to perform the receiver coordinate translation of the non-central receivers on each cluster. The translated coordinates for each cluster are averaged together using the truncated mean algorithm resulting in one set of latitudes and longitudes for each cluster. The moving average filter is applied to the latitudes and longitudes of each cluster. Finally, Vincenty's inverse method is executed again on the manipulated coordinates to obtain the final baseline distance.

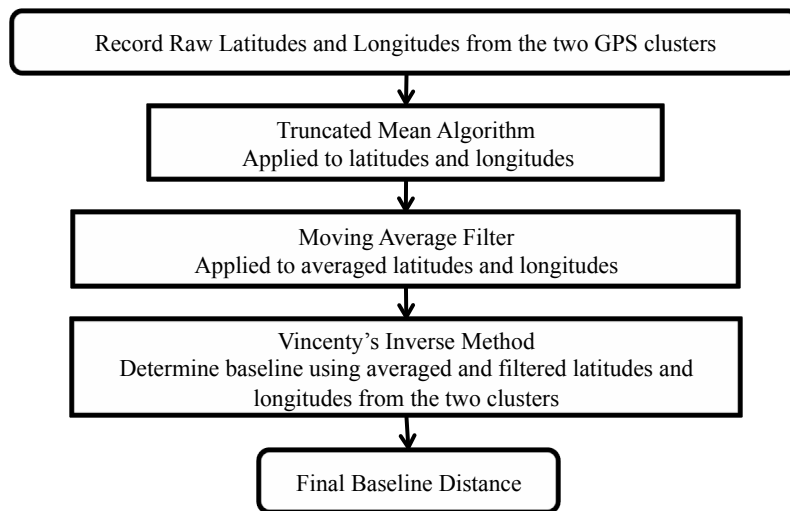


Figure 2.8. Averaging and Filtering Algorithm Flowchart

3. Hardware Implementation

This chapter introduces the hardware components used to assemble the base and rover data collection systems. In RTK GPS the term *base* defines the receiver from which RTK corrections are transmitted and *rover* for corrected GPS receiver. In this work, base and rover represents cluster one and cluster two respectively. Since GPS cost was one of the motivations of this work, a cost break down of the components is presented. The physical dimensions selected for the base and rover GPS receivers will be explained. Also, the raw data collection software that was developed in the C programming language will be explained.

3.1 Hardware Components

A cost breakdown of the Javad RTK system is given in Table 3.1. Included in the cost of the Javad receivers are specific features such as, 20 Hz update rate, 20 Hz RTK rate and advance multipath reduction, which increases the cost of the receivers. The Javad has two RS-232 communication ports on each receiver, one for transmitting or receiving RTK corrections and the second for spatial positioning of each receiver. The RTK corrections are transmitted via XBee-PRO RS-232 radio modems. Due to the many settings, each of the Javad receivers must be carefully configured to output the proper data.

Table 3.1.
Javad RTK system

Component	Quantity	Price (\$)
Javad Euro Receiver	2	13,870.00
Javad Marant+ L1/L2 Antenna	2	1,500.00
4 meter TNC Cable	2	50.00
Power Cable	2	30.00
Serial Cable	2	30.00
Xbee-PRO RS-232 Radio Modem	2	120.00
Total Cost: \$ 31,200.00		

Improper receiver settings can result in a decrease of accuracy. The receivers were programmed to output National Marine Electronics Association (NMEA) character strings GPRMC, GPGGA, and GPGSV once per second. These NMEA strings were recorded and used for further analysis. The NMEA strings contain the satellite information, calculated positioning, time and other information. The system was also programmed to operate in RTK mode, yielding the highest baseline accuracy. The RTK mode has different settings depending on the motion of the receivers. If the base receiver remains stationary, it can be set to extrapolate the RTK correction. Alternately, if both receivers are moving, the base receiver must be set to time synchronize so there is not a decrease in baseline accuracy. The Javad RTK system used in this thesis was originally purchased in 2003, when the technology was relatively new and expensive. A comparable system purchased at the writing of this thesis would cost around \$16,000.00.

Table 3.2.
Multiple GPS system

Component	Quantity	Price (\$)
Base: Garmin GPS Receiver #GPS 16x HVS	5	110.00
Rover: Garmin GPS Receiver #GPS 16x HVS	5	110.00
Total Cost: \$ 1,100.00		

The GPS receivers used for the post processing algorithm are inexpensive, compact, and ruggedly package receivers from Garmin. The receivers feature an integrated antenna, enabled WAAS corrections for higher accuracy, and RS-232 serial communication. Upon power up and a short warm up time, the Garmin receivers automatically start transmitting NMEA character strings GPRMC, GPGGA, GPGSA, GPGSV and the Garmin specific PGRMT string once per second, further discussed in Section 3.3.3. Unlike the Javad RTK system, the Garmin receivers do not require programming to operate correctly, which simplifies the setup. The approximate price and quantity of Garmin receivers is given in Table 3.2.

The number of receivers used for the base and rover were selected as a tradeoff between sample size, cost, and difficulty of implementation. As the number of receivers increases, the cost and ease of implementation decreases and begins to detract from the research goals.

Another consideration with either the Javad RTK or the multiple GPS system is what type of recording equipment to use. Two PC/104 computer stacks were selected for the raw data collection. A PC/104 is a single board computer in a small form factor commonly used in embedded computing applications. A variety of operating systems can be installed on the PC/104. The Microsoft DOS 6.20 operating systems was used in this thesis due to the very close to real time operation, small installation size, and low cost.

Table 3.3.
Data Recording Equipment used for Base and Rover

Component	Quantity	Price (\$)
PC/104 Processor Board, ICOP #VDX-6357	2	450.00
PC/104 Multi I/O Board, Winsystems #PCM-MIO-G-1	2	350.00
PC/104 Quad RS-232 Board, ICOP # ICOP-1800	2	70.00
PC/104 DC/DC Power Supply, Winsystems #PCM-HE104-G	2	209.00
12v 7Ah sealed Lead Acid Battery	2	20.00
3.5 inch Floppy Drive	2	5.00
Plastic Housing	2	7.00
Miscellaneous items	1	20.00
Total Cost: \$ 2,242.00		

A custom program written in the C programming language was developed to collect the raw GPS data, further details are given in Section 3.3. Additional functionality can be added by purchasing add-on boards which stack onto the PC/104 board. A breakdown of components used and approximate cost is given in Table 3.3.

Three additional boards were used for each of the two PC/104 stacks. The Multi I/O board adds analog and digital I/O capability, and was used to flag when a data set was ready to be collected and also to save an open data set to the hard disk and begin a new data set. The quad RS-232 board was used to acquire data from the Javad RTK receiver and five Garmin receivers. The DC/DC power supply regulated and conditioned the power for the PC/104 stack. The remaining items were supporting equipment for the data acquisition system.

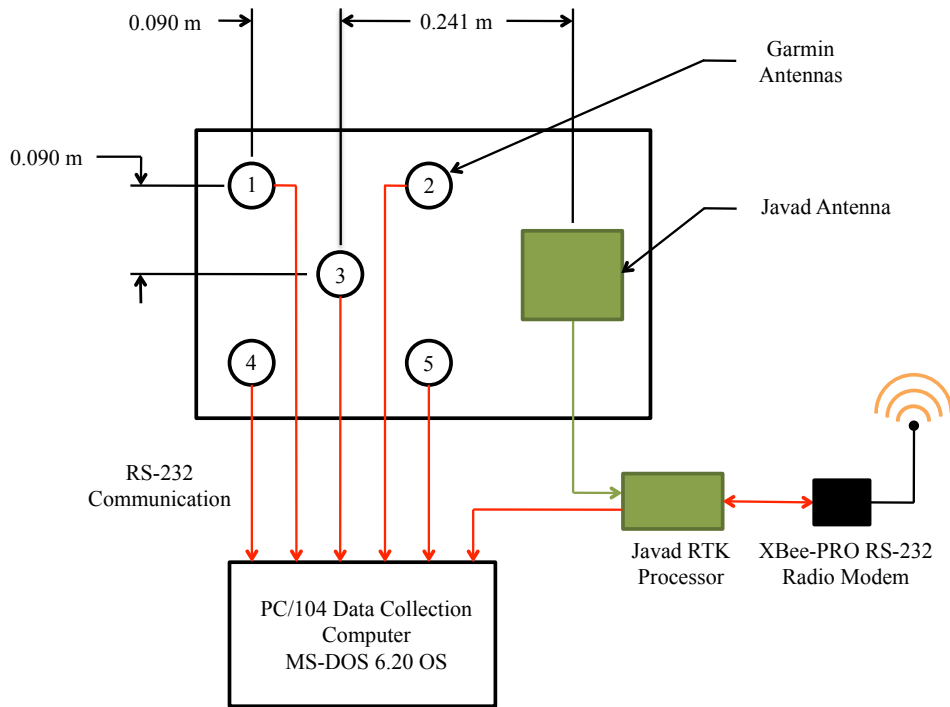


Figure 3.1. Data Collection Block Diagram for each Cluster

3.2 Physical Dimensions of Multiple GPS System

The physical layout of the multiple receiver system was designed to be compact, symmetrical, and easy to transport. A block diagram of both the base and rover is shown in Figure 3.1. An X-pattern was selected to simplify the translations corrections for the multiple Garmin receivers, with the spacing set to allow each receiver full view of the sky. The Javad antenna was also mounted on the same plate as the Garmin receivers, allowing direct result comparison. Also shown in Figure 3.2, is the XBee-Pro RS-232 radio modem, used for the Javad RTK correction communication.

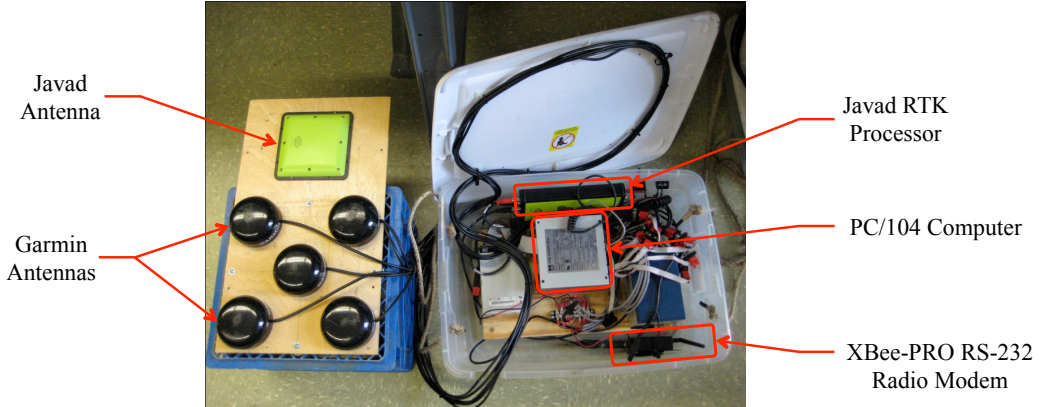


Figure 3.2. Actual Equipment Setup for each Cluster

The actual data collection apparatus is shown in Figure 3.1. On the left side of the Figure, the black circular objects are the Garmin receivers mounted to a wooden plate. The Javad antenna is also mounted to the same plate. Repeatable locating of the antennas during subsequent testing was a concern, leading to a low tech solution which as to mount the antennas to a plastic crate. On the right side of the figure, the data recording equipment is located inside of a plastic container. At the center of the container is the PC/104 stack enclosed inside a steel box to reduce electrical interference from interfering with the GPS reception. A floppy drive is mounted on the left side of the PC/104, used for retrieving data. The 12v sealed lead acid battery is mounted on the right side of the PC/104, providing power to all onboard components. At the top, the Javad RTK receiver is mounted. Next to the Javad receiver are two I/O switches used to flag and save off data sets. Finally at the bottom of the container is the XBee-PRO RS-232 radio modem, used for RTK communication.

3.3 Data Recording Program

Each of the PC/104 computers was setup to automatically begin recording GPS data when power was applied. A data recording program written in the C programming language was developed to work on either the base or rover devices. The program can be broken into five main components which are RS-232 communication, analog and digital I/O, Parsing GPS strings, Automatic Data file Handling, and a user display. The following is a brief overview of each of these main components

3.3.1 RS-232 Communication

A total of six low level RS-232 communication drivers were developed to handle the incoming GPS information. The program used an interrupt driven approach in conjunction with circular buffers to store the data between the raw collection, parsing, and storage.

3.3.2 Analog and Digital I/O

While recording data, it is often convenient to flag a given data set, making further processing easier. Analog and digital I/O drivers were developed for this purpose.

3.3.3 Parsing GPS Data Strings

A brief overview of the information contained in the NMEA 0183 version 2.00 ASCII strings will be given.

The Garmin receivers transmit the GPRMC, GPGGA, GPGSA, GPGSV and PGRMT strings once per second. Due to the amount of information contained in the NMEA strings, a parsing algorithm was developed to only save off only the first three strings, GPRMC, GPGGA, and GPGSV from the Garmin receivers. The Javad RTK system can be programmed to only output the three stings but the Garmin receivers cannot be programmed to only transmit select strings. The format of each NMEA strings is given below and specific definitions are given in Tables 3.4 through 3.6.

\$GPRMC,(1),(2),(3),(4),(5),(6),(7),(8),(9),(10),(11),(12)*nn [1]

\$GPGGA,(1),(2),(3),(4),(5),(6),(7),(8),(9),M,(10),M,(11),(12)*nn [1]

\$GPGSA,(1),(2),(3),(3),(3),(3),(3),(3),(3),(3),(3),(3),(3),(4),(5),(6)*nn [1]

Three example NMEA strings are shown below, the excluding the checksum.

\$GPRMC,221119,A,4322.3921,N,08336.5024,W,000.0,000.0,261110,007.2,W

\$GPGGA,221119,4322.3921,N,08336.5024,W,2,10,0.8,206.4,M,-35.3,M,,,

\$GPGSA,A,3,02,05,07,10,15,16,18,21,0,29,30,0,1.5,0.8,1.2

The GPRMC is the minimum recommended set of GPS information, GPGGA is the GPS fix data, and GPGSA is used for dilution of position and number of active satellites. Dilution of precision is a measure of the error associated with the GPS solution, but was not incorporated in the algorithms used in this thesis. The checksum, nn, is a validity check of the data contained between the “\$” and “*” characters, which can be used to ensure proper data transfer.

The NMEA strings set the quantization level of the receivers by limiting the significant digits in the latitude and longitude measurements. For example, the Garmin receivers latitudes and longitudes in the format ddmm.mmmm and dddmm.mmmm respectively, where “d” is degrees and “m” is minutes. The quantization level can be determined in meters using Vincenty’s inverse method by selecting an initial point and then varying the final point by the minimum quantization in both coordinate directions. The resulting Garmin Quantization is 0.1852 meters in the latitude direction and 0.1351 meters in longitude direction. The Javad receivers use NMEA 0183 version 2.3 ASCII strings which are a slightly updated from 2.0 version. The biggest difference being the latitudes and longitudes are recorded with higher precision. For example, the Javad RTK system transmits latitudes and longitudes as dd.mm.mmmmmmm and ddd.mm.mmmmmmm respectively. This results in much finer quantization, resulting in $1.852e^{-4}$ and $1.348e^{-4}$ meters in the latitude and longitude directions.

3.3.4 Automatic Data File Handling

In order to limit data file size, a counter was used to trigger auto saving and new file initialization. The counter was set to the maximum number of lines that would fit on a single floppy disk. Once the maximum is reached, the open data file is saved off, the file name incremented, and a new data file is opened. Testing on the algorithm made sure that no data was lost during this process.

Table 3.4.
GPRMC String Definition [1]

Item	Definition	Format
(1)	Time Stamp, UTC	hhmmss
(2)	Status	A = position valid, V = position invalid
(3)	Latitude	ddmm.mmmm
(4)	Latitude hemisphere	N or S
(5)	Longitude,	dddmm.mmmm
(6)	Longitude hemisphere	E or W
(7)	Speed over ground	000.0 to 999.9 knots
(8)	Course over ground	000.0 to 359.9 degrees
(9)	Date of position fix	ddmmyy
(10)	Magnetic variation	000.0 to 180.0 degrees
(11)	Direction magnetic variation	E or W
(12)	Mode	A = Autonomous, D = Differential, E = Estimated, N = Invalid data
nn	Checksum	ASCII

3.3.5 User Display

To ensure that data was being collected properly, a user display was developed to show the information being saved to the data file. This allowed for an instant check on the status of the data collection. At each test, a monitor was connected to the data collection computer at the beginning and at the end of the test to ensure proper operation.

Table 3.5.
GPGGA String Definition [1]

Item	Definition	Format
(1)	Time Stamp, UTC	hhmmss
(2)	Latitude	ddmm.mmmm
(3)	Latitude hemisphere	N or S
(4)	Longitude	dddmm.mmmm
(5)	Longitude hemisphere	E or W
(6)	GPS quality indicator	0 = Fix unavailable, 1 = non-DGPS fix, 2 = DGPS fix, 6 = Estimated
(7)	Number of satellites in use	00 to 12
(8)	Horizontal dilution of precision	0.5 to 99.9
(9)	Antenna height ± mean sea level	-9999.9 to 99999.9 meters
(10)	Geoidal height	-999.9 to 9999.9 meters
(11)	DGPS data age	seconds since last valid transmission (null if non-DGPS fix)
(12)	Differential Reference Station ID	0000 to 1023, (null if non-DGPS fix)
nn	Checksum	ASCII

Table 3.6.
GPGSA String Definition [1]

Item	Definition	Format
(1)	Mode	M = Manual, A = Automatic
(2)	Fix type	1 = unavailable, 2 = 2D, 3 = 3D
(3)	Satellite PRN number used in solution	01 to 32
(4)	Position dilution of precision	0.5 to 99.9
(5)	Horizontal dilution of precision	0.5 to 99.9
(6)	Vertical dilution of precision	0.5 to 99.9
nn	Checksum	ASCII

4. GPS Testing and Algorithm Results

In this chapter, the results of three types of tests are described to investigate the use of multiple GPS receivers to improve relative distance measurements. In all cases a high accuracy Javad RTK GPS system was also used for comparison. Short duration stationary tests were conducted at several baseline distances each for 60 seconds. A long duration stationary test was also performed at a fixed baseline for 73 minutes. Three mobile tests were conducted where the GPS clusters and the Javad RTK base and rover were fixed to a moving vehicle with a baseline distance of 4.48 m.

4.1 Short Duration Stationary Testing

4.1.1 Test Objective

Short duration stationary testing was conducted to determine the two cluster GPS baseline distance accuracy for several distances. The hypothesis was that for short time durations the GPS errors would be equally distributed bias errors between each pair of GPS receivers with negligible frequency content. For short durations, the Ionosphere and Troposphere error, would be considered constant in time and depend on baseline distance.

Additionally ephemeris and satellite clock errors were expected to cancel since both clusters would use the same set of satellites. However, receiver noise was not expected to be constant between the receivers in each cluster. Under these assumptions, the averaging and filtering algorithm should result a zero mean baseline error.

4.1.2 Test Plan and Procedure

Short duration, 60 seconds, stationary testing was conducted by collecting latitude and longitude data at increasing baseline distances, from 7.62 to 91.44 meters in 7.62 meter increments. The cluster orientation, increment, and test setup are shown in Figure 4.1. The test was conducted in an open field with a clear view to the sky in all directions on a straight and level paved road. A photograph of the test site is shown in Figure 4.2. In order to maximize test repeatability, a grid was painted on the road. The grid distances were measured using a fiberglass surveyor tape measure long enough to layout the entire grid in one setup, minimizing error stack-up. During the test, cluster one was fixed at zero meters and cluster two was manually moved to the different baseline distances. Data was collected for 60 seconds at each location, starting at 7.62 meters and ending at 91.44 meters, with 30 seconds allotted after each relocation, allowing the relocation transients to smooth out. If the receivers were tipped during the manual relocation, some number of satellites in view might be lost. Therefore care was taken to keep the cluster level during the manual relocation.

Several sources of error were identified for the short duration stationary testing. The grid used to mark the baseline locations had possible errors with the conservative estimate of ± 0.05 meters. It is also likely that the measurement errors increase with distance due to using a fiberglass tape measure which can be stretched under tension.

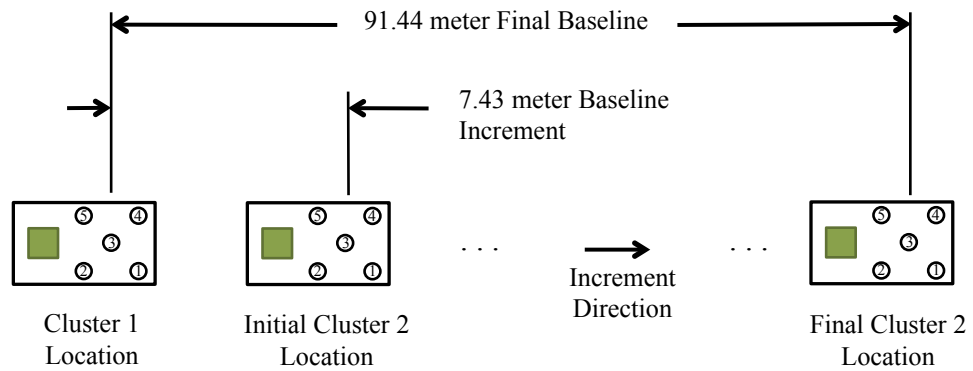


Figure 4.1. Short Duration Stationary Test Setup

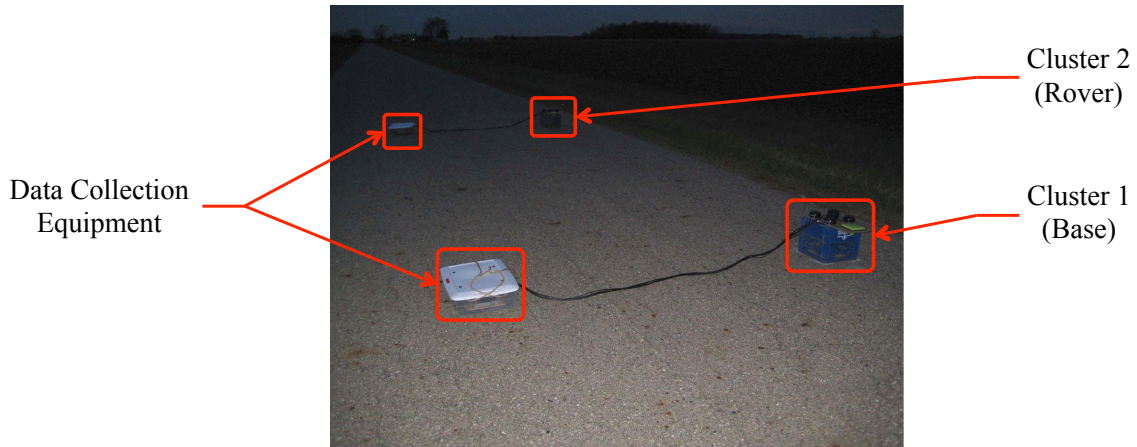


Figure 4.2. Actual Short Duration Stationary Test

The linearity of the grid is also accounted for in the error estimate. Another source of error is the angular relationship between the two clusters and is estimated to be within $\pm 5^\circ$. Angularity error would effect the receiver coordinate translation, but the effect is small because the small radial distance of the X-pattern configuration between the multiple receivers.

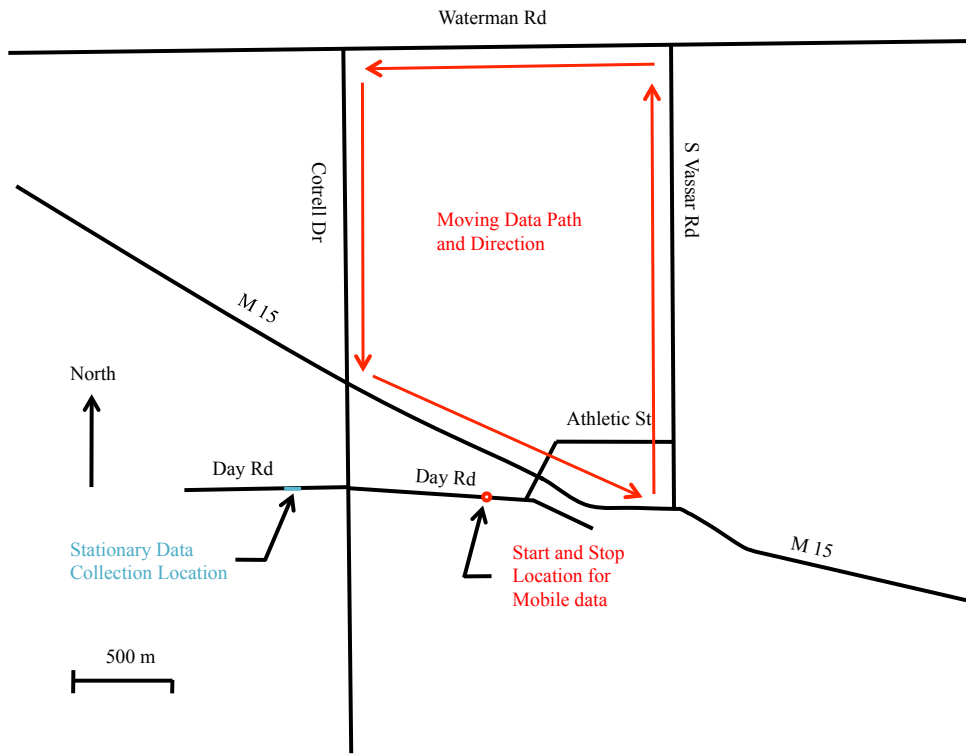


Figure 4.3. Map Showing Locations where Stationary and Mobile Data was Collected

The two short duration stationary tests were conducted near Vassar Michigan, with the approximate coordinates of 43.372° latitude and -83.595° longitude. A map showing the test locations is shown in Figure 4.3. The mobile testing location is also shown on the map and is further discussed in Section 4.3.

4.1.3 Short Duration Results

The short duration results are shown in several ensuing plots as time averaged cluster-to-cluster baseline distance errors. The baseline error was calculated by subtracting the measured distance from the baseline calculated using Vincenty's Inverse method described in Section 2.1. Each data point represents 60 seconds of time averaged data at each distance.

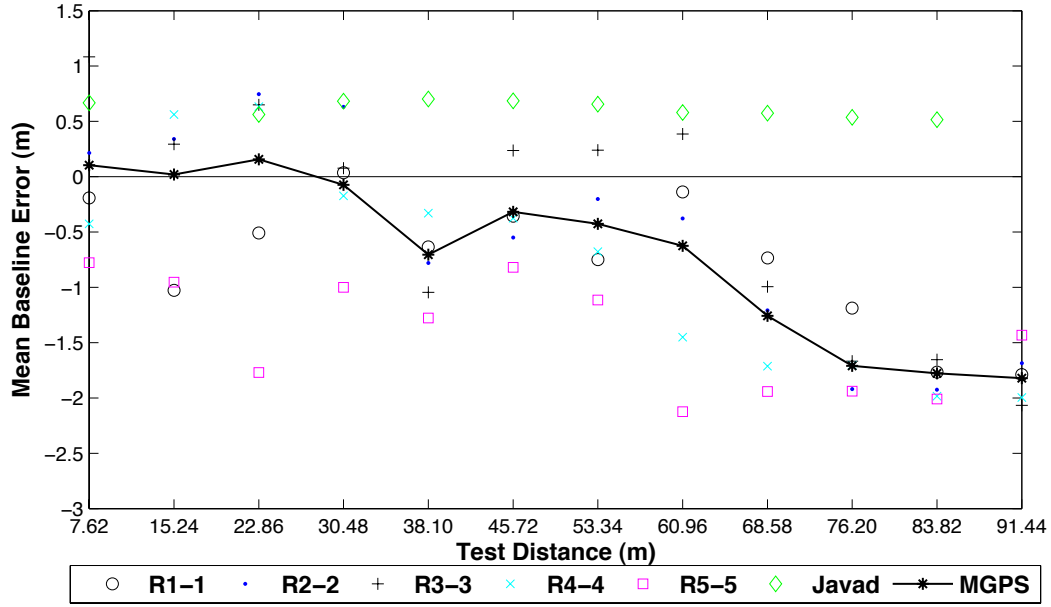


Figure 4.4. Time Average Short Duration Stationary Test, Baseline Error, Test 1, 25 Nov 2010, Start Time = 190417 UTC

This allows trends to be shown in the data that would be more difficult to see in time domain data. Results from the first test are shown in Figure 4.4.

The Javad RTK system results are shown as the green diamond markers. The Javad results do not show centimeter accuracy as expected by an RTK GPS system. It is likely an incorrect receiver setting caused the decrease in performance related to the data format for the RTK correction and the RTK update rate. The data was still included, but conclusions could not be drawn from this data set. Data points at 15.24 and 91.44 were omitted due to erroneous data caused by tipping the clusters during the manual relocation.

In Figure 4.4, the raw baseline distances are shown as R1-1 through R5-5 which corresponds to the matching pairs of receivers in each cluster. For example R3-3 is the raw baseline distance between cluster one and two using the coordinates of receiver three.

The term "raw" referrs to baseline distances calculated from the un-processed coordinates from a unique pair of receivers using Vincenty's Inverse method.

The results from the multiple GPS (MGPS) system employing the post processing algorithm are shown as the black line with asterisks defining each data point. The MGPS solution depends on the five R_{i-i} measurements, and is therefore bounded by them. The overall trend of the MGPS distance estimates is an increasing bias error as baseline distance increases. The increasing error matches what is expected from a DGPS system. The data also suggests that the best accuracy is obtained in baselines under 30 meters. The main reason for the increasing error with baseline is the conditions at the two clusters become increasingly uncorrected with larger baselines. Furthermore, the different atmospheric conditions at each cluster could contribute to the bias error at large baseline distances. There is no data at baseline distances larger than 91.44 meters to determine if the increasing bias trend continues or levels out to a steady-state value. The effect of the truncated mean averaging can be seen very well at 22.86 meters, where a spread of 2.5 meters occurs.

The MGPS system results in near zero baseline error at this data point, suggesting receiver noise plays a large role in baseline accuracy. However, if all the raw data points are tightly group, such as at 83.82 meters, the averaging does little to the result. Furthermore, when all the raw data is biased, then averaging does not yield improved results.

The short duration stationary test was conducted a second time to determine system repeatability, with the results shown in Figure 4.5. The raw Garmin results in test two are not as accurate as test one. As a result, the MGPS system was also less accurate. The baseline results to be evenly distributed at each baseline interval, but the results are biased. Another observation is that the receiver pairs showing the worst error do not continue to show this behavior at every interval.

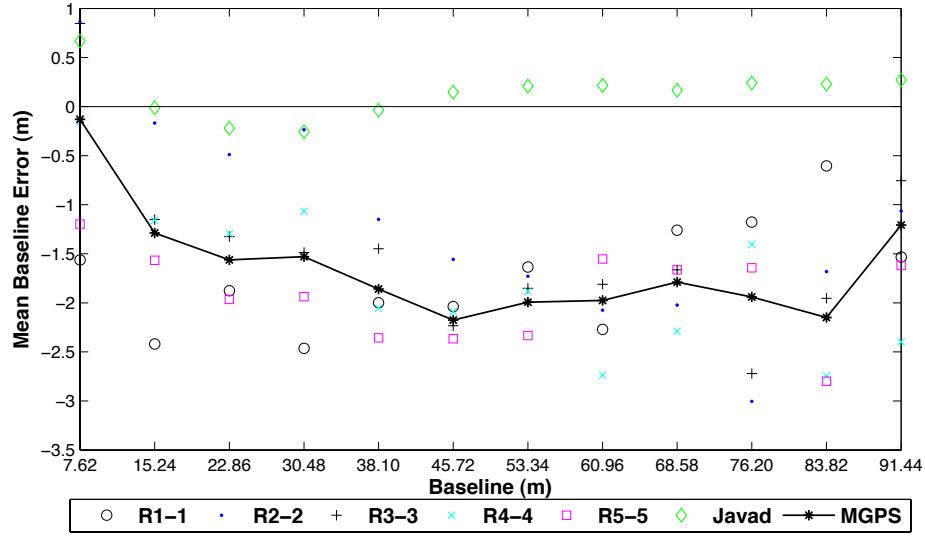


Figure 4.5. Time Averaged Short Duration Stationary Test, Baseline Error, Test 2, 25 Nov 2010, Start Time = 213618 UTC

For instance, receiver pair, R1-1, gives is the worst estimate at 15.24 m and the best estimate at 83.82 m . This shows that sensor pairs do not contain a failed sensor and that receiver noise plays a large role. The trend of the MGPS system while similar to test 1, falls steeply after the 7.62 meter baseline distance and then drops slowly to roughly a 2 meter baseline error. The final baseline distance shows a slight up trend in accuracy, but there is not enough data to change the overall trend. The Javad RTK system shows improved accuracy which approaches the reported centimeter accuracy and is consistent through the entire test. No changes were done to the Javad receiver settings during the two short duration tests or the long duration test.

The results of the MGPS system and Javad RTK system from short duration tests one and two are overlaid in Figure 4.6. The overall trend for the MGPS system shows increasing bias error as baseline distance increases while the Javad RTK system shows constant or near constant bias. The MGPS system also shows baseline distance error under 2.5 m which grows with baseline distance.

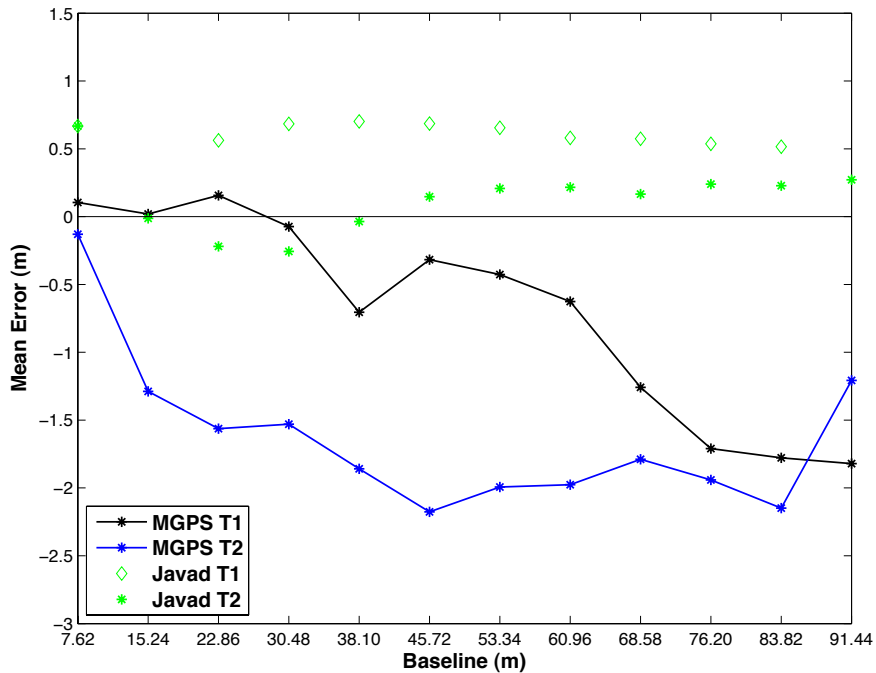


Figure 4.6. Time Averaged Short Duration Stationary Test, Baseline Error, Multiple GPS System, Tests 1 - 2

4.2 Long Duration Stationary Testing

4.2.1 Test Objective

The long duration stationary testing was conducted to characterize the baseline error at a fixed baseline distance of 45.72 meters for 73 minutes, performed similarly to the short duration testing. The hypothesis is that the baseline errors will be caused mainly by receiver noise and also by the atmosphere due to the baseline distance.

4.2.2 Test Plan and Procedure

The long duration stationary test was conducted similarly to short duration testing using the same grid and orientation as shown in Figure 4.1. Latitude and longitude data was collected from both clusters for a total of 73 minutes. The two clusters were given a startup time of two minutes before collecting data to allow for startup transients.

4.2.3 Long Duration Results

The results of the long duration test are shown in Figure 4.7, which includes raw, MGPS system, and Javad RTK baseline errors. The stair step patterns in the raw baseline distance errors show the quantization level of the Garmin receivers which is approximately 0.1 meters. Similar to the short duration results, averaging of biased data does not improve the MGPS system accuracy. It is not clear as to why overall MGPS trend shows a decreasing baseline error as run time increases with a 1500 second period oscillation.

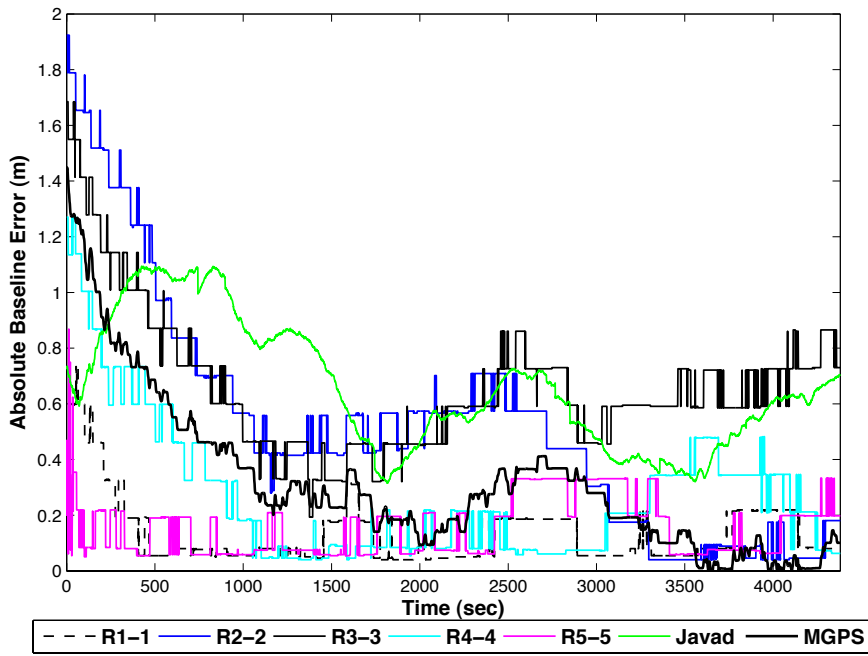


Figure 4.7. Long Duration Stationary Test, 45.72 meter Baseline, 29 Nov 2010, Start Time = 161853 UTC

The slow component of WAAS correction would correct the position over two to six minutes, which is not consistent with the 16 minute feature in the data. Other possible explanations for this behavior are sensor temperature changes effecting receiver noise, long duration start up transients, and atmospheric anomalies.

The Javad RTK results do not show a significant difference in accuracy between the short duration and long duration tests which both lack centimeter accuracy. The Javad receiver settings were not changed between two types of tests, further suggesting an error in the receiver settings. The Javad results were still included but conclusions could not be drawn from them.

4.3 Mobile Testing

4.3.1 Test Objective

The main focus of this thesis is having both clusters in motion while attempting to estimate relative distance. The hypothesis is that the mobile data will yield results different from the two types of stationary testing due to multipath errors and changing atmospheric conditions caused by the motion of the clusters. As in the stationary cases, the receiver noise will be an error source.

4.3.2 Test Plan and Procedure

The mobile testing was conducted on a set route near the stationary data collection site as shown in Figure 4.3. A test vehicle was outfitted with a mounting apparatus for the two clusters that locked both the orientation and baseline distance to 4.483 meters, as shown in Figures 4.8 and 4.9. The baseline distance and orientation were accurate to 0.002 meters and $\pm 2^\circ$ respectively. Three separate mobile tests were performed by collecting data while driving around the set course. Each test lasted between 20 and 40 minutes while the vehicle speed was varied from 0 to 18 m/s dynamically to allow for starts and stops along the course. The course had a combination of urban and rural terrain, all of which had a clear view of the sky. However, some areas had objects taller than the antenna height which could have caused multipath errors. The Javad RTK system was programmed to allow dynamic motion of both receivers with high accuracy.



Figure 4.8. Actual Mobile Test Vehicle

4.3.3 Mobile Results

The mobile test results are presented in two forms for the three tests. The first is a comparison between the MGPS system and the Javad RTK output and the second is comparing the worst case Garmin result with the MGPS system. The worst case Garmin results were calculated by finding the pair of GPS receivers with the largest baseline distance error at each time step. The worst case results are given as absolute values of baseline distance error. Finally the MGPS results from the three tests are overlaid to show overall trends.

The mobile results from test one through three, comparing the MGPS system and Javad RTK system, are shown in Figures 4.10 through 4.13. The MGPS system shows varying baseline error above and below zero, as shown in Figure 4.10, which suggests the multiple GPS approach improves the results. The remaining results are shown as absolute baseline distance errors.

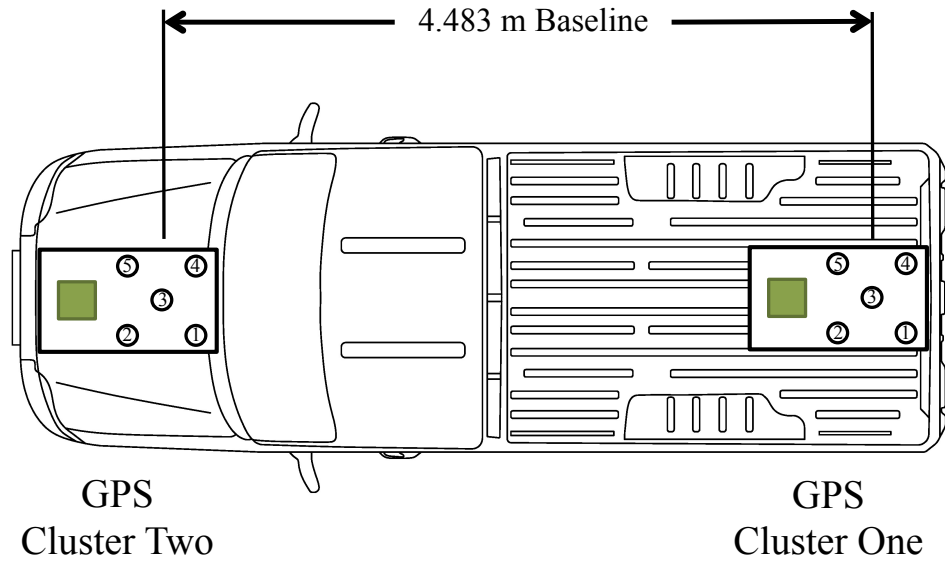


Figure 4.9. Mobile Test Vehicle Setup

The Javad RTK system can resolve the baseline distance to centimeter accuracy for much of the test. However, large baseline distance excursions sometimes occur when the Javad RTK system loses lock to a single or multiple satellites, which can be seen on Figure 4.11 near $t = 400$ seconds. The maximum baseline distance excursions from the Javad RTK system were 9.42, 7.26, and 10.94 meters for tests one through three respectively. Alternately, the MGPS system had much better performance with maximum baseline distance excursions with values of 1.15, 1.85, and 1.20 meters for the same tests.

The improvement in GPS performance using multiple GPS receivers compared to a single receiver pair is shown in Figures 4.14 through 4.16. A worst case scenario was developed by picking the pair of receivers between the two clusters that resulted in the largest baseline error at each time step. A considerable increase in performance was seen in all three the tests

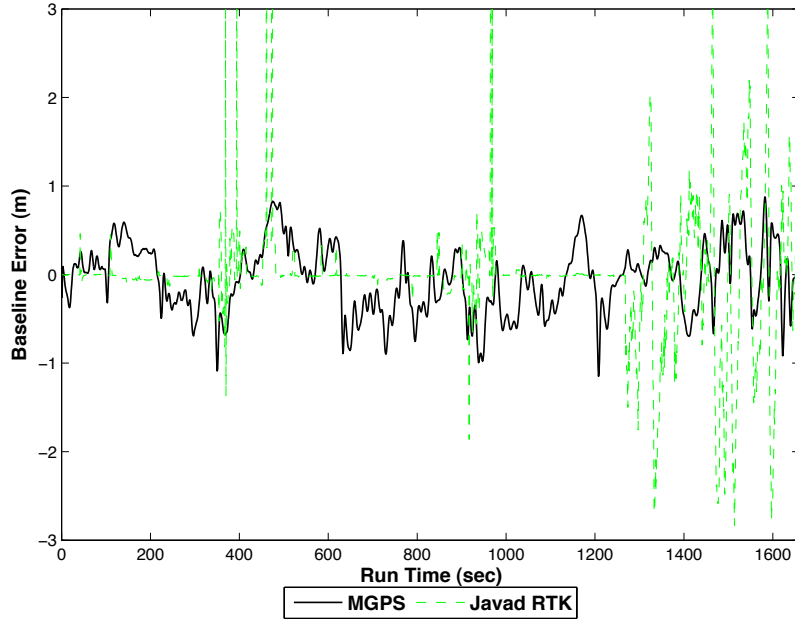


Figure 4.10. Mobile Test 1, Multiple GPS System and Javad RTK Comparison, 4.48 m Baseline, 29 Dec 2010, Start Time = 193648 UTC

Overlaying the MGPS system results from tests one though three is shown in Figure 4.17. The results show test consistency with a majority of the baseline distance errors below one meter. Overall, the MGPS system performs reliably in the mobile application by showing less sensitivity to losing satellite lock than the Javad RTK system and improved performance when compared to a worst case pair scenario.

The mobile tests results were examined using three statistical measures of performance; the mean, two standard deviations (2σ), corresponding to a 95% confidence interval, and the root mean square (RMS) baseline distance error, shown as Equations 4.1 through 4.3. The results of these measures are shown in Tables 4.1 through 4.4. The Javad RTK system was analyzed using the whole data set and also a subset of 250 consecutive data points selected where the large baseline excursions were minimal. Table 4.1 shows the MGPS system is capable of sub-meter accuracy 95% of the time for two of the three mobile tests.

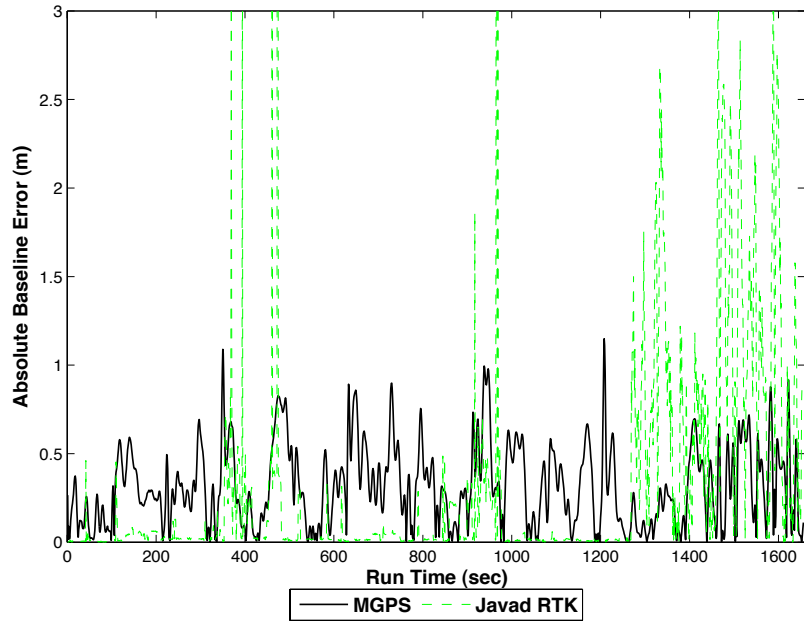


Figure 4.11. Mobile Test 1, Multiple GPS System and Javad RTK Comparison, 4.48 m Baseline, 29 Dec 2010, Start Time = 193648 UTC

$$\mu = \frac{1}{n} \sum_{i=1}^n x_i \quad (4.1)$$

$$\sigma = \sqrt{\frac{\sum_{i=1}^n (x_i - \mu)^2}{n-1}} \quad (4.2)$$

$$x_{rms} = \sqrt{\frac{x_1^2 + x_2^2 + \dots + x_n^2}{n}} \quad (4.3)$$

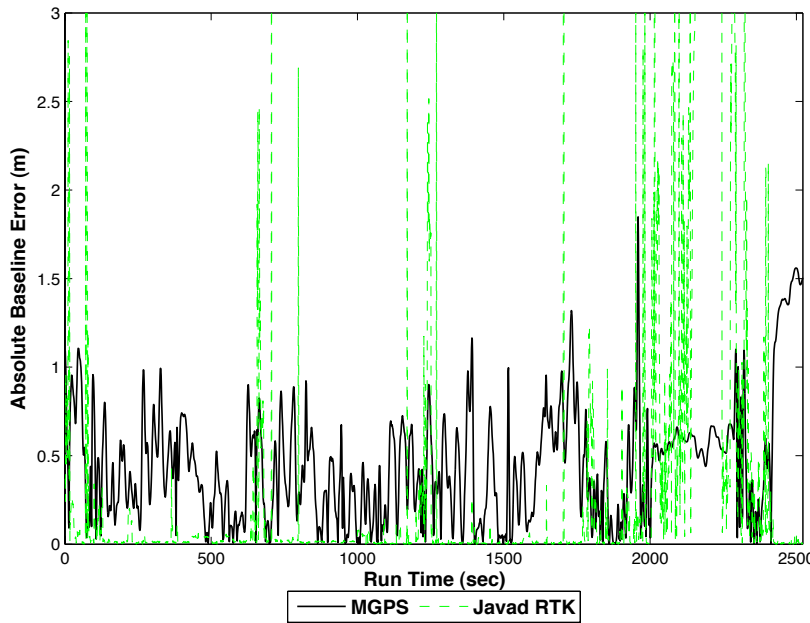


Figure 4.12. Mobile Test 2, Multiple GPS System and Javad RTK Comparison, 4.48 m Baseline, 29 Dec 2010, Start Time = 22502 UTC

The RMS errors show the GPS baseline varies under 0.6 meters for all three mobile tests. The MGPS results are far superior to the worst case scenario, shown in Table 4.2. The mean baseline distance errors approach 3.2 meters for the first two tests with better results on test three. The 2σ values show errors larger than the three meter estimated accuracy of the WAAS correction. The RMS errors show large variations in the baseline distance errors with values around three to five meters. Statistically, when considering the entire data set the Javad RTK results are not superior to the MGPS results, as shown in Table 4.3. The large excursions experienced by the Javad RTK muddle the results. Therefore a partial data set was selected to show typical RTK GPS performance, as shown in Table 4.4. The partial results show the RTK system is capable of millimeter accuracy for the mean and centimeter accuracy in baseline distance 95% of the time.

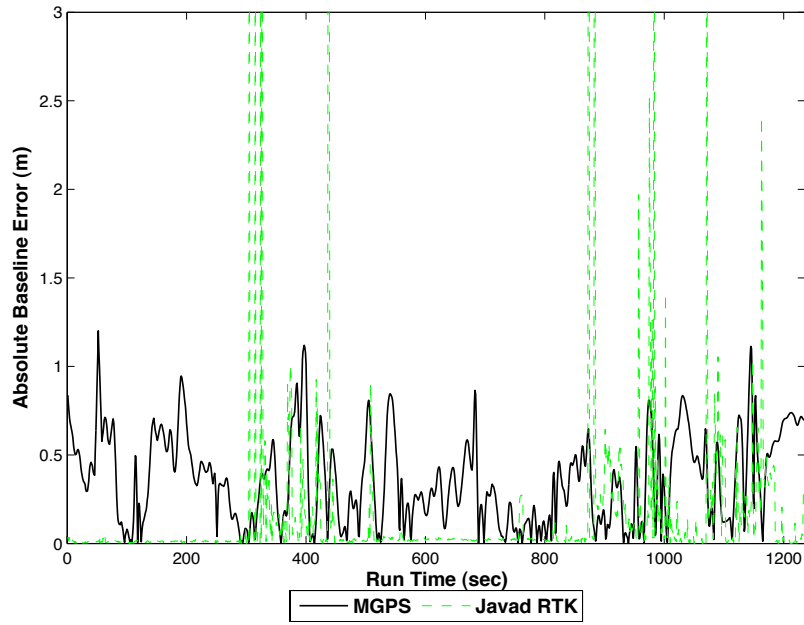


Figure 4.13. Mobile Test 3, Multiple GPS System and Javad RTK Comparison, 4.48 m Baseline, 30 Dec 2010, Start Time = 150311 UTC

Table 4.1.
Statistical Mobile Test Results - Multiple GPS System - Full Data Set

Test	Mean (m)	2σ (m)	RMS Error (m)
1	-0.0572	0.7681	0.3882
2	-0.0744	1.1072	0.5585
3	-0.0731	0.8659	0.4389

Table 4.2.
Statistical Mobile Test Results - Worst Case GPS Pair - Full Data Set

Test	Mean (m)	2σ (m)	RMS Error (m)
1	-3.1227	7.9488	5.0535
2	-3.0502	4.6331	3.8299
3	-1.9713	6.1000	3.6305

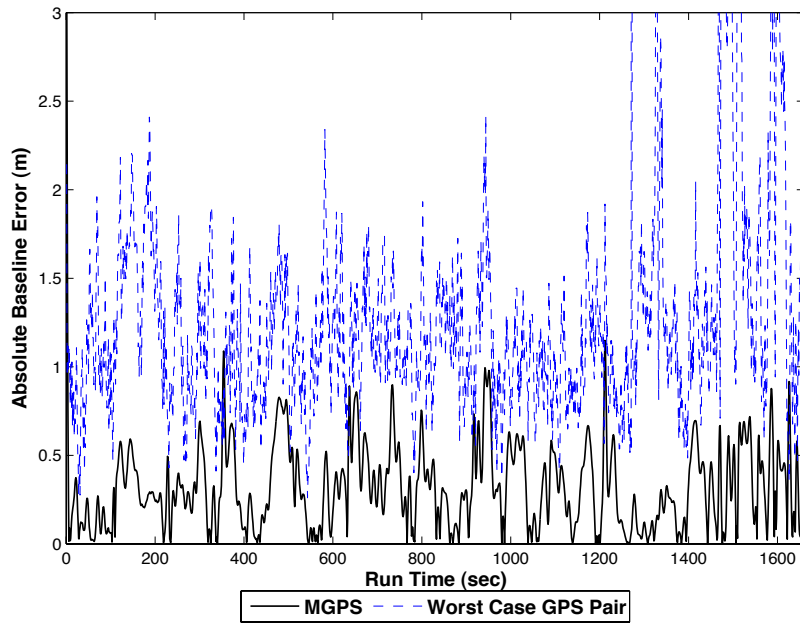


Figure 4.14. Mobile Test 1, Absolute Error Comparison, 4.48 m Baseline, 29 Dec 2010, Start Time = 193648 UTC

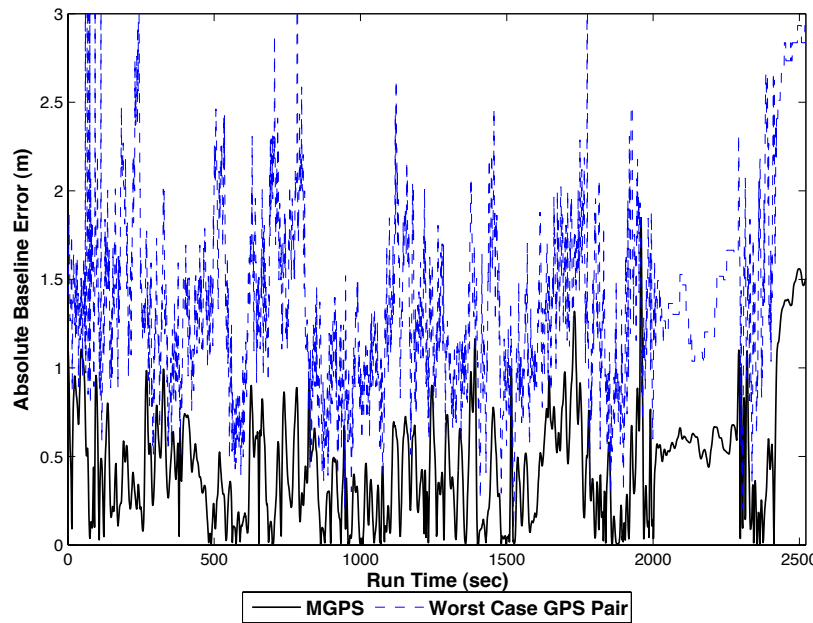


Figure 4.15. Mobile Test 2, Absolute Error Comparison, 4.48 m Baseline, 29 Dec 2010, Start Time = 22502 UTC

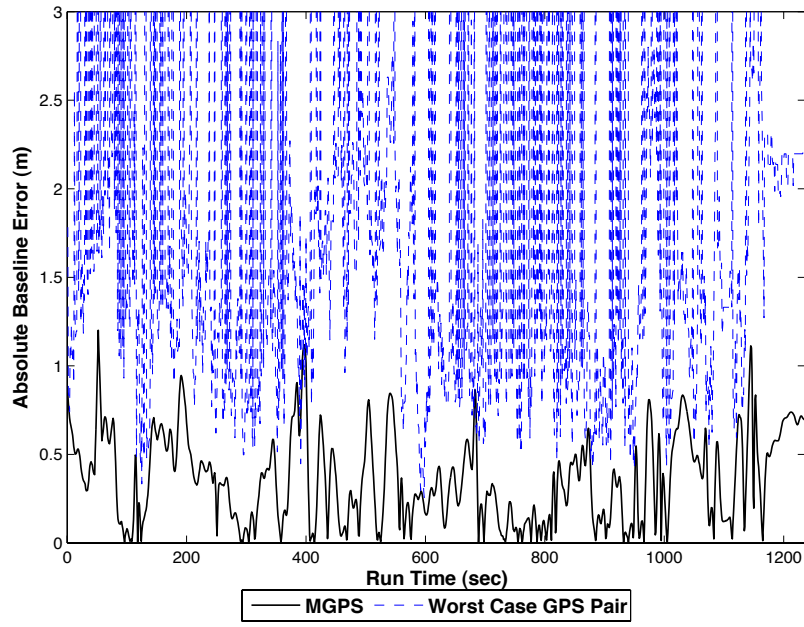


Figure 4.16. Mobile Test 3, Absolute Error Comparison, 4.48 m Baseline, 30 Dec 2010, Start Time = 150311 UTC

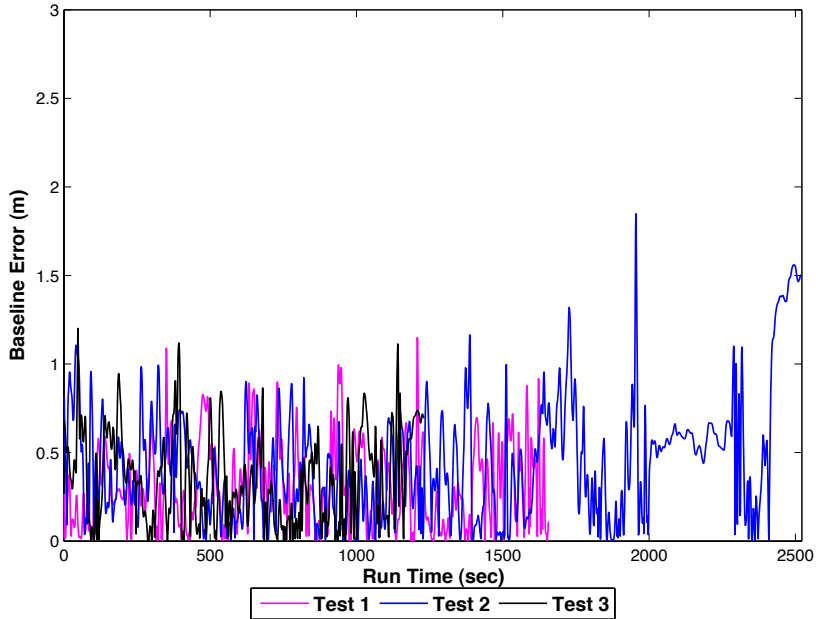


Figure 4.17. Mobile Test Comparison of Multiple GPS system, Tests 1 - 3, 4.48 m Baseline

Table 4.3.

Statistical Mobile Test Results - Javad RTK System - Full Data Set

Test	Mean (m)	2σ (m)	RMS Error (m)
1	-0.0211	1.4958	0.7480
2	0.2252	2.0935	1.0705
3	0.0631	1.3287	0.6671

Table 4.4.

Statistical Mobile Test Results - Javad RTK System - Partial Data Set

Test	Mean (m)	2σ (m)	RMS Error (m)	Data Points
1	-0.0077	0.0263	0.0152	990-1240
2	-0.0034	0.0428	0.0170	1285-1535
3	-0.0262	0.0832	0.0491	550-800

5. Summary, Conclusions, and Future Work

5.1 Summary

An overview of GPS operation was given along with a description of its error sources. The different augmentations to increase GPS accuracy were also discussed, such as DGPS, WAAS, RTK GPS and post processing. A post processing algorithm was developed to increase baseline distance accuracy using two clusters of inexpensive GPS receivers. A truncated mean averaging technique was applied to each cluster to reject outliers in the raw coordinates and provide a single set of coordinates for each cluster. A moving average filter was used to smooth the coordinates from each cluster, reducing noise. Vincenty's Formulae were described and the inverse method was used to calculate baseline distance. Two data collection devices were constructed to collect GPS data in stationary and mobile settings. Accuracy comparison was performed between the multiple GPS system and the Javad RTK system. Three different types of tests were conducted to test the performance of each GPS system. The first test was a short duration stationary scenario to determine accuracy as a function of baseline distance. The second was a long duration stationary test, used to determine the long period behavior of the GPS. The third test had both clusters moving and was the main focus of this research.

5.2 Conclusions

The data acquired from the Javad RTK system during the stationary tests was erroneous due to incorrect receiver settings. It is plausible that if the stationary tests were repeated with correct receiver settings, the baseline accuracy from the Javad RTK system would be equivalent to its performance in the mobile tests.

The MGPS system showed an inverse dependence between baseline distance and accuracy in the short duration tests. This matches the behavior of a DGPS system. Thus baseline distances should be limited depending on the accuracy required.

The MGPS system was able to obtain baseline accuracy of approximately one meter in the mobile application, and had accuracy superior to the Javad RTK system when satellite lock was lost causing a large excursion in baseline error. One meter accuracy is a 200% increase in performance from the receiver specifications. This is not because five receivers were used. The actual averaging was performed with the three most consistent measurements. The main conclusion is that multiple low cost GPS receivers can be used to improve accuracy of relative position measurements.

The MGPS system baseline accuracy was less sensitive to loss of satellite signals as compared to the Javad RTK system. The Javad RTK system was shown to yield centimeter accuracy 95% of the time in the mobile application if the baseline excursions were not included.

Although more receivers could further improve the accuracy, centimeter accuracy is impossible due to the limited number of latitude and longitude significant digits in the receiver data packet. This suggests that inexpensive GPS receivers were not designed for centimeter level accuracy, as provided by an RTK GPS system.

5.3 Future Work

The number of GPS receivers used in each cluster could be increased, which would increase the sample size for the truncated mean. The overall system cost could also be kept constant by purchasing less expensive chip type GPS receivers in larger quantities. The existing data set could be used to investigate other sensor number scenarios including single though five.

A more advanced averaging technique could be developed that would determine which data points are outliers based on a given tolerance, taking better advantage of small sample sizes.

The coordinate translation could be implemented using additional orientation sensors for both clusters. This would allow for both increased cluster size and to used more accuracy GPS receivers based on quantization level.

Other methods for determining accurate baseline distances could be implemented allowing for height differences between the two clusters. Vincenty's direct and inverse methods do not account for height differences in the calculation, limiting the application.

The MGPS system could be modified for realtime execution, making it applicable for control of dynamic systems.

Other filtering techniques could be applied other than the moving average filter implement in this thesis. For example, the Kalman filter could be used with additional sensors to develop a more complete navigation strategy using a multiple GPS approach.

REFERENCES

- [1] *GPS 16x Technical Specifications*, Garmin International, Inc., 1200 E. 151st Street Olathe, KS 66062 USA, September 2008.
- [2] J. B. Tsui, *Fundamentals of Global Positioning System Receivers a Software Approach*. New York, NY: Wiley, 2000.
- [3] T. Logsdon, *The Navstar Global Positioning System*. New York, NY: Van Norstrand Reinhold, 1992.
- [4] E. D. Kaplan, Ed., *Understanding GPS: Principles and Applications*. Norwood, MA: Artech House, 1996.
- [5] P. H. Dana. (May 2000) The geographer's craft project, department of geography, the university of colorado at boulder. [Online]. Available: http://www.colorado.edu/geography/gcraft/notes/gps/gps_f.html
- [6] R. B. Langley, "GPS receiver system noise," *GPS World*, vol. 8, no. 6, pp. 40–45, 1997.
- [7] S. Nair, "A multiple antenna global positioning system configuration for enhanced performance," M.S. thesis, Dept. Elect. Eng., Athens OH, Ohio Unin, 2004.

- [8] T. Vincenty, “Direct and inverse solutions of geodesics on the ellipsoid with application of nested equations,” *Survey Review* 23, pp. 88–93, April 1975.
- [9] G. Lu *et al.*, “Performance analysis of a shipborne gyrocompass with a multi-antenna gps system,” in *Position Location and Navigation Symposium, 1994, IEEE*, Apr. 1994, pp. 337–343.
- [10] K. J. Turner and F. A. Faruqi, “Multiple gps antenna attitude determination using a gaussian sum filter,” in *TENCON '96. Proceedings. 1996 IEEE TENCON. Digital Signal Processing Applications*, 1996, pp. 323–328.
- [11] R. A. Nayak *et al.*, “Analysis of multiple gps antennas for multipath mitigation in vehicular navigation,” in *Institute of Navigation National Technical Meeting*, Anaheim, CA, January 26-28 2000.
- [12] S. Hong *et al.*, “Estimation of errors in ins with multiple gps antennas,” in *Industrial Electronics Society, IECON '01. The 27th Annual Conference of the IEEE*, 2001, pp. 410–415.
- [13] C. Yoo and I. Ahn, “Low cost gps/ins sensor fusion system for uav navigation,” in *Digital Avionics Systems Conference, 2003. DASC '03. The 22nd*, 2003, pp. 8.A.1–1 – 8.A.1–9.
- [14] A. Marazzi and C. Ruffieux, “The truncated mean of an asymmetric distribution,” *Computational Statistics & Data Analysis*, pp. 79–100, 1999.
- [15] S. W. Smith, *Digital Signal Processing: A Practical Guide for Engineers and Scientists*. Burlington, MA: Newnes, 2003.

Appendix A: Raw Data Figures

The raw data used to determine the time averaged stationary data for test one is shown in Figure A.1. The large baseline excursions of the Javad are due to tipping the cluster during manual relocation.

The multiple GPS system and Javad system are compared in Figure A.2. The MGPS system shows high accuracy at shorter baselines but decreases at further distances.

The raw results of short duration stationary test two are shown in Figures A.3 and A.4. Similar trends are observed between tests one and two where the Javad excursions are due to tipping of the receiver during relocation. The performance of the MGPS system was less than observed in test one.

The raw latitudes and longitudes were plotted to show the actual path traveled during mobile test one in Figure A.5. From a macroscopic view, the MGPS and Javad RTk system show little difference in the path traveled. The figure also shows the start and stop locations as the short "J" shaped portion of the path located near the bottom of the figure. Also, the smaller rectangle in the lower right of the course was the path used to return from the testing.

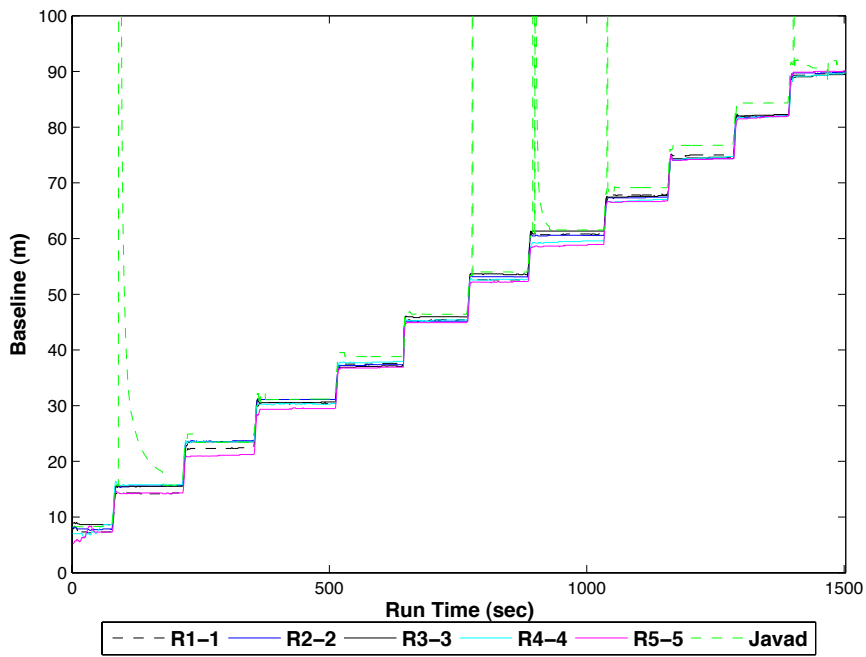


Figure A.1. Short Duration Stationary, Raw Baselines, 7.62 - 45.72 meters, Test 1

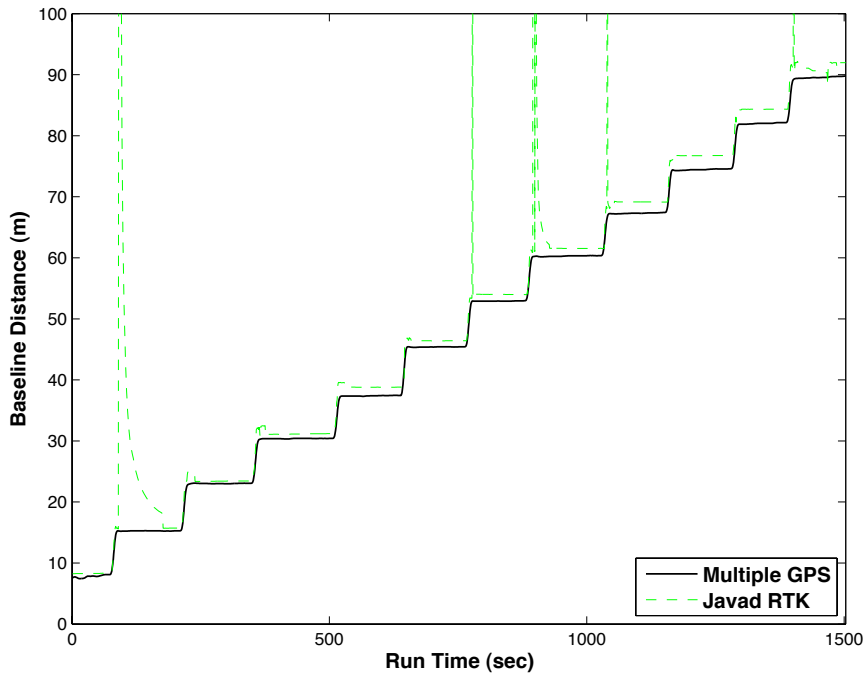


Figure A.2. Short Duration Stationary, Baseline comparison, 7.62 - 45.72 meters, Test 1

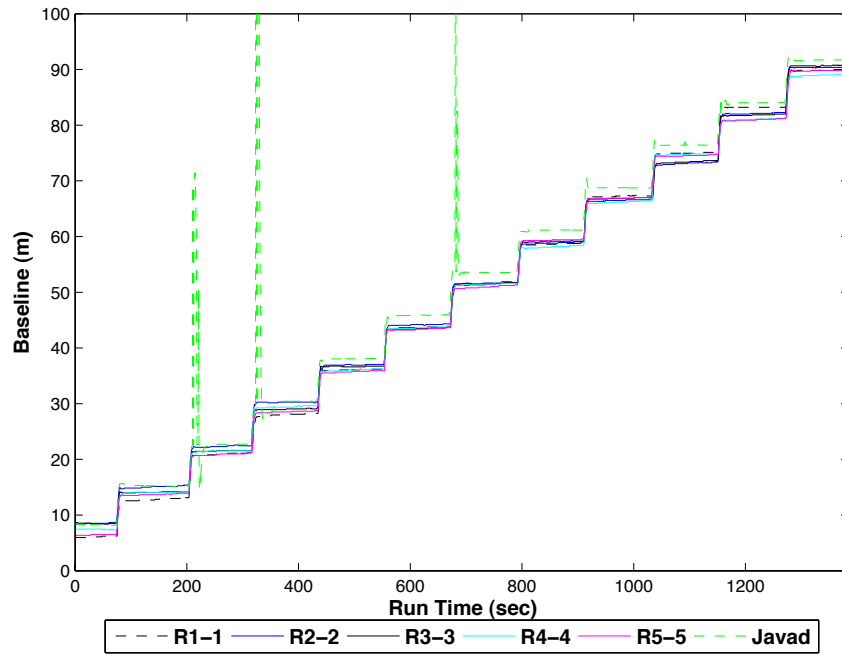


Figure A.3. Short Duration Stationary, Raw Baselines 7.62-45.72 m, Test 2

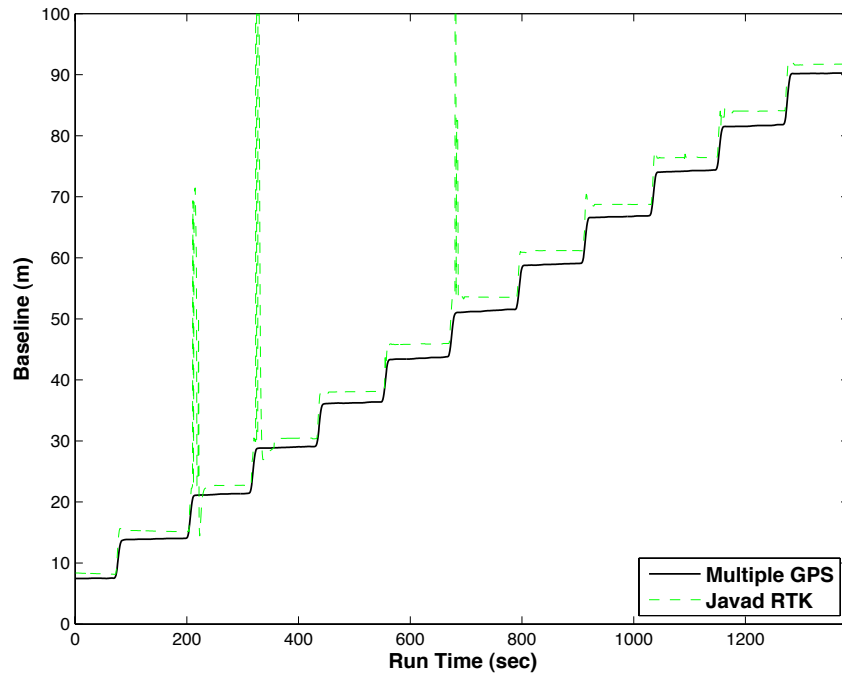


Figure A.4. Short Duration Stationary, Baseline comparison 7.62-45.72 m, Test 2

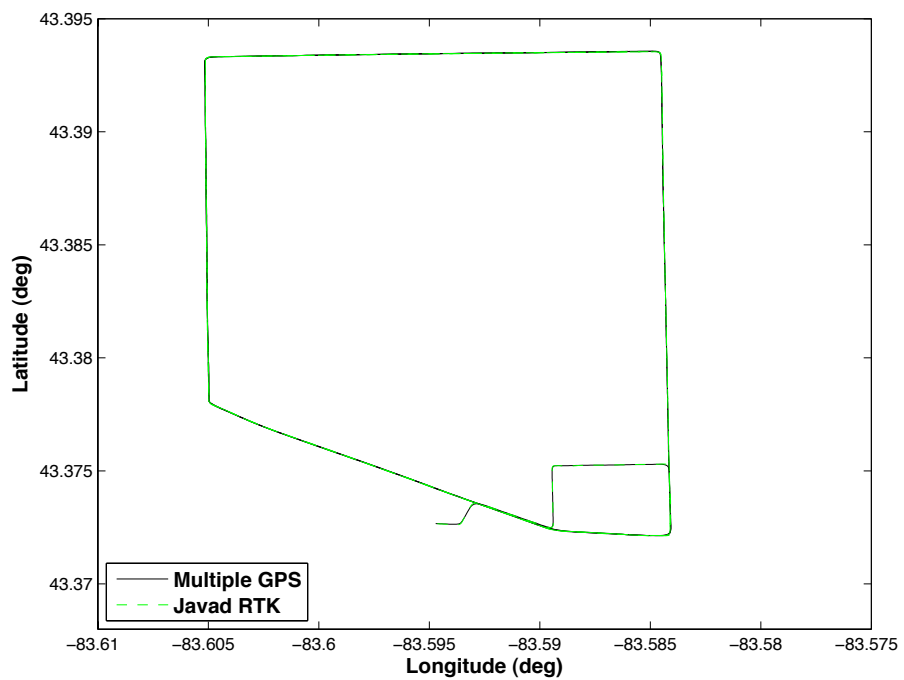


Figure A.5. Mobile Test 1, Latitude vs. Longitude, Cluster 2 Data